



**“Isolation and analysis of single bacterial cell using a
microfluidic device”**

*Major Project-II Submitted in Partial Fulfillment of the
Requirement for the Degree of*

Master of Technology

In

Biomedical Engineering

Submitted by

ASADULLAH

(DTU/14/M.TECH/102)

Under the supervision of

Prof. B.D Malhotra

Department of Biotechnology

Delhi Technological University, Delhi

Shahbad Daulatpur

Main Bawana Road

New Delhi, Delhi 110042.

CERTIFICATE



This is to certify that the M. Tech. dissertation's report of major project-II entitled "Isolation and analysis of single bacterial cell using a microfluidic device", submitted by Asadullah(DTU/14/M.Tech/102) in partial fulfillment of the requirements for award of the degree of Master of Technology, Biomedical Engineering, Delhi Technological University (Formerly Delhi College of Engineering, University of Delhi), is an authentic record of the candidate's own work carried out by him under my guidance. The information and data enclosed in this dissertation is original and has not been submitted elsewhere for honoring of any other degree.

Prof. B. D. Malhotra

Professor
Department Of Biotechnology
Delhi Technological University
Shahbad Daulatpur
Delhi -110042

Prof. D. Kumar

Head of the Department
Department Of Biotechnology
Delhi Technological University
Shahbad Daulatpur
Delhi -110042

DECLARATION

I declare that my report of major project-II entitled *Isolation and analysis of single bacterial cell using a microfluidic device* submitted to Department of Biotechnology, Delhi Technological University is authentically carried out by me.

Date: 22 /07/2016

Place: Delhi

ASADULLAH

ACKNOWLEDGEMENT

First of all I would also like to thank my principal guide Prof. B.D. Malhotra for his willingness and kind permission to allow me to work in THSTI, Faridabad.

Then, I would like to thank my co-guide Dr. Jonathan Pillai for giving me an opportunity to perform my major-II project in his esteemed laboratory and also for constantly motivating and beautifully guiding me that has been of immense help to me in accomplishing this project so far.

I am also truly thankful to Dr. Jonathan Pillai, Dr. Pallavi, Dr. Krishnamohan Atmakuri and their lab members who helped me in completing this project.

My special thanks goes to the SIIP fellows especially Mr. Sumit Kumar, who helped me in learning Solid WorksTM designing.

I would also like to extend my gratitude to Dr. Feroz at C-Camp Bangalore for helping me with the microfabrication.

Thanks are due to the administration staffs of Dept. of Biotechnology, DTU and THSTI for their constant support.

I am greatly and honestly thankful to my parents and other family members who provided me with all the other necessary requirements and their invaluable constant moral support that helped me in completing this project.

ASADULLAH

Roll no.:2K14/BME/04

Regn. No.: DTU/14/M.Tech/102

TABLE OF CONTENTS

1. Abstract
2. Introduction
3. Literature Review
4. Introduction to Microfluidics
 - 4.1. Laminar Flow
 - 4.2 Inertial Microfluidics
 - 4.3 Diffusive mixing.
5. Fabrication Methods for Microfluidic Devices
 - 5.1. Photolithography
 - 5.2. Soft Lithography
6. Initial Prototyping
7. Computer Aided Design
 - 7.1. Solid Modeling
 - 7.2. Auto CAD Designs.
8. Materials and methods
 - 8.1. Preparation of bacterial Culture.
 - 8.2. FITC staining of bacteria for live cell imaging.
 - 8.3. Agarose Pad Microscopy.

9. Results and discussion.

10. Proof of Concept.

10.1. Evaluation of Bacterial Growth Under Normal Growth Conditions.

10.2. Evaluation of Bacterial Growth Under 25 $\mu\text{g/ml}$ Kanamycin in LB medium.

10.3. Evaluation of Bacterial Growth Under 50 $\mu\text{g/ml}$ Kanamycin in LB medium.

11. Conclusions and Future Directions.

12. References.

LIST OF FIGURES AND TABLES

SERIAL NO.	DESCRIPTION
Figure 2.1	Pictorial representation of microfluidic toolbox
Figure 2.2	Pictorial representation of generation of mycobacterial daughter cells of unequal length.
Figure 4.1	Dimensional Considerations.
Figure 4.2	Particle experiencing inertial focusing in a microchannel.
Figure 4.3	Representative image for focusing of particles in narrowest dimension.
Figure 5.1	Fabrication procedure for a single layer microfluidic device.
Figure 5.2	Pictorial representation of Soft lithography process.
Figure 6.1	Designing of Micro pattern using slides and cover slips.
Figure 6.2	Flow of coloured water in micro channels.
Figure 6.3	Micropattern showing the central chamber adapted for mixing of fluid.
Figure 6.4	The design showing the position of the pillars
Figure 7.1	Sketches and solid model views of Design no.1
Figure 7.2	Sketches and solid model views of Design no.2
Figure 7.3	2D sketches of features of Design No.3.
Figure 7.4	The complete assembled design no.3 in isometric 3D view.
Figure 7.5	2D sketch of inlet, outlet chambers and connectors to the central chamber to enable dynamic mixing of input fluids.
Figure 7.6	Completely assembled (3D Isometric view) of fourth design after rendering in Solid Works™.
Figure 7.7	Snapshots of AUTOCAD designs in gerber file

	viewer of first design.
Figure 7.8	Annotated images of AUTOCAD designs in gerber file viewer of second design.
Figure 7.9	Annotated images of AUTOCAD designs in gerber file viewer of third design.
Figure 7.10	Images of AUTOCAD designs in gerber file viewer of fourth design.
Figure 8.1	FITC molecular structure.
Figure 8.2	Pictorial Representation of the mould preparation process.
Figure 8.3	Pictorial representation of the PDMS casting process.
Figure 9.1	Fluorescent microscopy images of Bacterial Smear showing the FITC stained <i>Mycobacterium</i> at 40X.
Figure 9.2	Fluorescent microscopy images of <i>Mycobacterium</i> bacteria on an agarose pad at 40X.
Figure 9.3	Types of Agarose pads used in this experiment.
Figure 9.4	Images of the PDMS devices cast from the master moulds, taken by high resolution photography.
Figure 9.5	Bright field microscopy images of central chamber of all the four designs at 4X magnification.
Figure 9.6	Image of the complete Device no.3 with inlet and outlet tubings.
Figure 9.7	Fluorescent microscopy images in a microfluidic device.
Figure 10.1	Fluorescent microscopy images at 40X of FITC stained <i>E.coli</i> under normal LB medium.
Figure 10.2	Fluorescent microscopic images of <i>E.coli</i> under Kanamycin (25 µg/ml) containing

	medium in the device at 40X.
Figure 10.3	Fluorescent microscopic images of E.coli under Kanamycin (25 µg/ml) containing medium in the device after 30 minutes at 40 X.
Figure 10.4	Fluorescent microscopic images of <i>E. coli</i> (O.D.- 0.2) under Kanamycin (50µg/ml) containing medium in the device at 40 X.

TITLE

“Isolation and analysis of single bacterial cell using a microfluidic device”.

Asadullah, Department Of Biotechnology, Delhi Technological University, Delhi.

E-mail: asadullah4edu@gmail.com.

Chapter 1. ABSTRACT

Tuberculosis (TB) is one of the major reasons of mortality and morbidity worldwide. Its treatment involves a battery of antibiotics to be administered to the patient for 6-9 months. As a result of this prolonged treatment, the mycobacterium undergoes two phases of cell death firstly an initial phase of quick cell death and then a refractory phase of delayed cell death. Due to this refractory phase, some copies among a population of bacteria called as persisters, may develop tolerance or resistance to antibiotics. The persisters are phenotypic variants in the same population. Currently, there is a lack of tools for the *in vitro* study and analysis of such phenotypic variants as most methods rely on identifying growth and apoptosis in a clonal population. As a result, there is a need for new tools that allows us to isolate and modulate the local environment of individual cells in clonal population to indentify and study the phenotypic variants. Therefore in this dissertation, I have used microfluidic devices as a platform technology for isolating single bacterial cells from a clonal population. These devices also allow us to present the bacterial with various environmental challenges, including treatment with different antibiotics. Finally, I have used fluorescent microscopy to study morphological changes in single *E. coli* cell upon treatment with different concentrations of kanamycin as a proof of concept of the ability of the microfluidic device platform to analyse single cells.

Chapter 2. INTRODUCTION

2.1 GENERAL

It is widely acknowledged that *Mycobacterium Tuberculosis* (*M Tb*) is one of the most successful pathogen on the planet, infecting one-third of the entire human population globally (Global tuberculosis report 2013, WHO, 2013). This bacterium has unusual way of asymmetric cell division, in which the daughter cells are of unequal sizes (Aldridge, B. B. et al, Joyce, G. et al. Singh, 2012. B. et al, Santi, I et al, 2013). This feature might have given a unique survival edge to the bacterium in the highly variable host environment (Karen J. Kieser et al, 2014). The growth rate and composition of the cell wall of the daughter cells are also different that leads to functional diversification in the population (Aldridge, B. B. et al, Joyce, G. et al. Singh, 2012. B. et al, Santi, I et al, 2013).

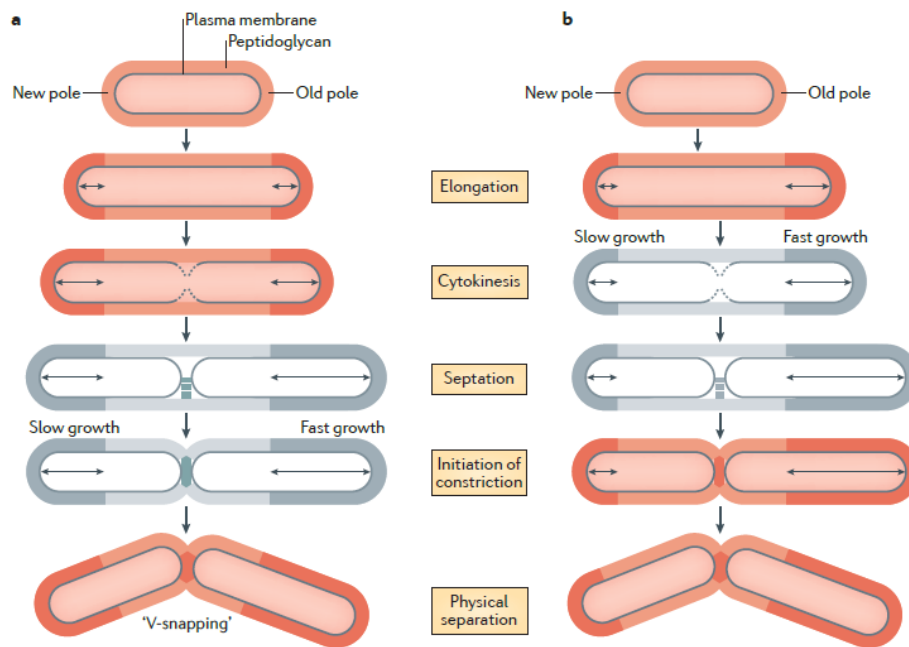


Figure 2.1: Pictorial representation of generation of mycobacterial daughter cells of unequal length. (Taken from Karen J Kieser et al, 2014).

The first model (Fig. 2.1.a) depicts that at the outset, both poles undergo equal growth and there is uniform elongation of the cell during cytokinesis. However, faster growth takes place at the old pole after cytokinesis, which leads to production of unequal sizes of daughter cells. The second model (Fig. 2.1.b) depicts that faster growth takes place in the old pole as compared to that of the new pole prior to cytokinesis itself, and is maintained throughout the subsequent cell

division process. In this case as well, the end result is that daughter cells of unequal sizes are generated

In addition to the above variation in growth, it may be noted that the treatment of *M. Tb* involving a battery of antibiotics to be administered to the patient for 6-9 months is another well documented source of phenotypic variation in the mycobacterium. As a result of this prolonged treatment, the mycobacterium undergoes two phases of cell death, viz., firstly an initial phase of quick cell death and then a refractory phase of delayed cell death. Due to this refractory phase, some copies among a population of bacteria, called as persisters, may develop tolerance or resistance to antibiotics (Nathalie Q. Balaban et al, 2004, Yuichi Wakamoto et al, 2013). The persisters are often phenotypic variants within the same population, potentially because of their individual response to minor variations and changes in the local environment of the colony (Nathalie Q. Balaban et al, 2004, Yuichi Wakamoto et al, 2013).

Currently, there is a lack of tools for the *in vitro* study and analysis of such phenotypic variants as most methods rely on identifying growth and apoptosis in a clonal population (i.e. in a colony or in a multi-well plate) with thousands of copies of the bacteria. As a result, there is a need for new tools that allows us to isolate and modulate the local environment of individual cells in clonal population to indentify and study the emergence of phenotypic variants.

As stated by the WHO, health care technology (diagnostics and therapeutics) in developing countries should be ASSURED (Affordable, Sensitive, Specific, User friendly, Rapid and robust, Equipment free, and Deliverable to end users) (Peeling, R. WHO programme on the evaluation of diagnostic tests. Bull. W. H. O. 2006). Lab-on-a-chip, MEMS-based diagnostics, drug delivery devices and single cell genomic and proteomics are some of the steps forward in fulfilling above requirement. All of these utilize microfabrication techniques such as electrowetting, optofluidics, di-electrophoresis, etc. whereby the use of a small sample volume and its accurate analysis is possible.

Microfluidics is a technology platform that uses sub- millimetre length scales and microlitre volumes, thus mitigating reagent usage and sample loss (Todd A. Duncombe et al, 2015). Microfluidic devices help in precisely controlling the fluid flow, because the flow in microfluidics is typically a laminar flow and not turbulent, and lacks eddies and vortices,

(Beebe, D. J et al, 2002). The patterning of laminar flow makes the fluid lamina of varying compositions adhere to specific channels of the device (Takayama, S. et al). The sub- millimeter scale chambers and channels help in hydrodynamic focusing of mammalian and bacterial cells (Anthony Tony, 2011) and as a result, microfluidics has wide application in cell and molecular biology studies.

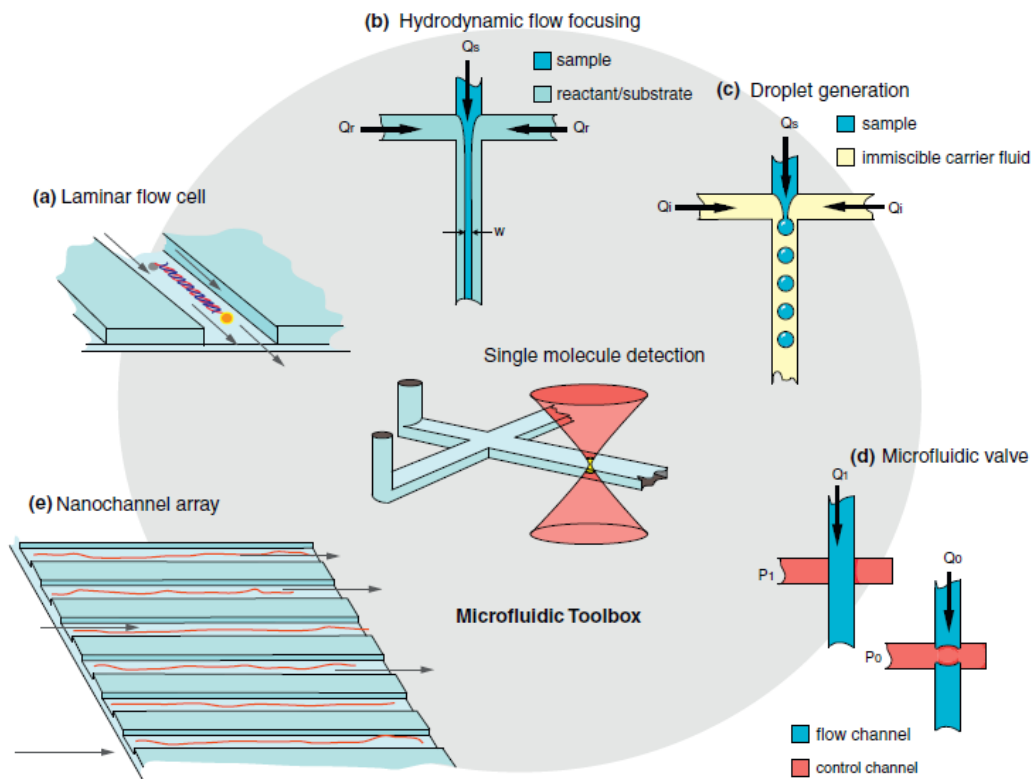


Figure 2.2: Pictorial representation of microfluidic toolbox. (a) Laminar flow in a single channel. A DNA molecule which is labeled and immobilized, shows stretching due to flow. (b) Hydrodynamic focusing. (c) Generation of droplets from the liquid sample solution. (d) A valve of micron size. (e) Arrays of nanosized channels that are used for optical mapping of DNA molecules. (f) Detection of single molecule. (Taken from Aaron M Streets et al, 2014).

With the eventual goal of studying the persistence phenomenon and emergence of phenotypic variations in *Mycobacterium tuberculosis*, a microfluidics platform has been developed in the current thesis to study the morphological variation in a single copy of the bacterium. However, for the purpose of establishing proof of concept, we have used *E. coli* as a model system to study the effect of various environmental challenges, including the effect of different concentrations of antibiotics.

Chapter 3. LITERATURE REVIEW

1. Ping wang et al (2010) had used microfluidic devices to study the long-term growth and division patterns of *Escherichia coli* cells. They had analyzed approximately 105 individual cells and came to the conclusion that the mother cell inheriting the same pole for hundreds of generation had a remarkable stability. They had shown that the death of *E. coli* is not random but due to accumulating damages. They conclude that the cell death is not related to robust growth of *E. coli*.
2. Christopher Probst et. al. (2013) had developed a microfluidic device with sub-micron sized barriers used to trap single *E.coli* cells and grow them. The cells were analysed to be viable and unaffected by the neighbouring cell. The debris was appropriately cleared by the fluid flow in the device without affecting the trapped bacteria. They had said that the device can be used for studies on prokaryotic cells, such as effect of pH, carbon sources, temperature and others.
3. Bree B. Aldridge et al (2012) had shown that physiologically distinct sub populations of *mycobacterial* cells arising through asymmetric growth and division exhibit different levels of drug susceptibility to tomeropenem, cycloserine, isoniazid and rifampicin. They had used a microfluidic device to trap and grow the bacteria and perform time-lapse imaging of the dividing bacterium, in order to conclude above mentioned fact.
4. Min Cheol Kim et al (2010) had developed a microfluidic device with ellipsoidal geometrical structures to trap single GFP expressing *E. coli* cells. The cells are trapped into a narrow aperture through hydrodynamics trapping. They have shown that their numerical simulation data matches with that of the microfluidic device experiments.
5. Ali Asgar S. Bhagat et al (2008) had developed a unique method to isolate particles in rectangular straight microchannels by applying the concepts of inertial microfluidics. They have shown that by increasing the aspect ratio of the channels and so the shear rate increases across the channel cross section that can help in focussing particles along the

vertical sidewalls, in a comparatively shorter microchannel length. This gives an edge to this design in various microfluidic applications.

6. Mahdokht Masaeli et al (2012) had successfully demonstrated the continuous filtration of particles that have different dimensions in X and Y axes by applying the concepts of inertial micro-fluidics. In this they have shown the relationship of particle aspect ratio to their equilibrium position in the microchannels. The separation of such non-spherical particles' dependency upon the Reynolds number, the flow rate and channel aspect ratio is also well illustrated in this work. Therefore, this finds an exemplary usage in designing devices for the isolation and separation of particles of biological or medical interest in which particles are not usually perfectly spherical or rectangular in geometry, as is the case with mycobacterium.

Chapter 4: MICROFLUIDICS

Microfluidics is the study of fluid dynamics at a micron or sub-micron scale ($\leq 10^{-6}$ m) level, in which micro to nano litres of fluid flows through microscopic channels (Whitesides GM, Nature 2006). The physical behaviour of fluids at the micron length scale is different from that which is observed in large channels. Gravity loses importance as the physical length scale of the system is miniaturised. Surface tension, Vander Waals forces and surface roughness are some of the types of surface forces that start dominating at the micron length scale (H. A. Stone et al, AIChE J., 47, 2001). Since the effect of viscous forces are more pronounced in micron chambers, the flow is typically laminar and the mixing of molecules takes place because of diffusion (T. M. Squires, et al, Rev. Mod. Phys. 77, 2005). This phenomenon helps in the study of the effect of stimuli on biological systems to the level of sub-cellular compartments (Takayama S, Ostuni, Chem Biol 2003).

Microfluidics finds wide application in the field of disease diagnosis where very small volume of sample gives specific results as compared to the traditional methods of sample analysis in a comparatively short time. Recent developments in this field have given rise to Lab-on-a-chip (LOC) or micro Total Analysis Systems (μ TAS) where microfluidic chambers are integrated with sensor systems.

Figure 4.1 below elucidates some basic concepts of microfluidics such as laminar flow, inertial microfluidics and diffusive mixing of different fluids.

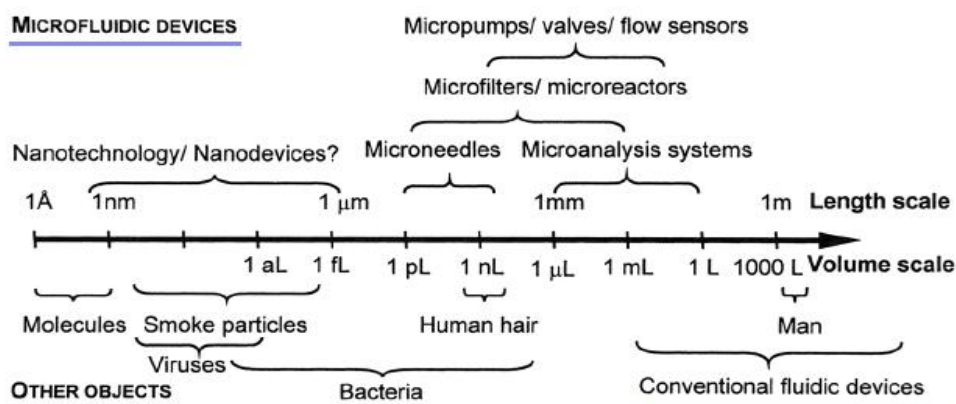


Figure 4.1: Dimensional Considerations (Taken from Nguyen, NT and ST Wereley, Fundamentals and Applications of Microfluidics, Artech House, Boston, MA).

4.1 Laminar flow:

In microfluidics, the surface-to-volume ratio is highly increased because of which physical properties of the fluid flow is affected and the friction forces dominate. This leads to the parallel flow of the layers of fluid with negligible currents perpendicular to the flow, leading to a layered flow of parallel lamina, thus giving it the name of “laminar flow”. The dimensionless Reynolds number (Re) describes the nature of the fluid flow that whether it is laminar or turbulent

$$Re = \rho v D_h / \mu \longrightarrow \text{Equation (1)}$$

Where,

ρ : the density,

v : flow velocity,

μ : viscosity

D_h : Characteristic length

Turbulent flows are indicated by high value of Reynolds number, ($Re > 2000$) and laminar flows are indicated by low value of Reynolds number ($Re < 2000$). In microfluidics, the Reynolds number is generally below 10 (Tabeling P, 2005).

4.2 Inertial Microfluidics:

Fluid flowing through a microchannel follows a parabolic flow path because the layer of the fluid that is in the centre of the channel has highest velocity as compared to the layer of the fluid along the walls (that is almost zero). So a particle in this flow experiences different velocity on each side of it. This difference in velocity is dependent upon the shape of the flow profile and the size of the particle. Now if this difference is large enough then the particle rotates and is pushed above towards the wall of the channels by a lift force, F_{LS} (Matas J et al, 2004). Once the particle reaches close enough to the channel wall, it will start experiencing a perpendicularly opposite lift force F_{LW} . Then the position of the particle in the flow is decided by the equilibrium position between the two opposite forces, F_{LS} and F_{LW} (Mach AJ, Bioeng. 2010, Segré G et al, Nature 1961, Di Carlo D et al, Physical Review Letters, 2009).

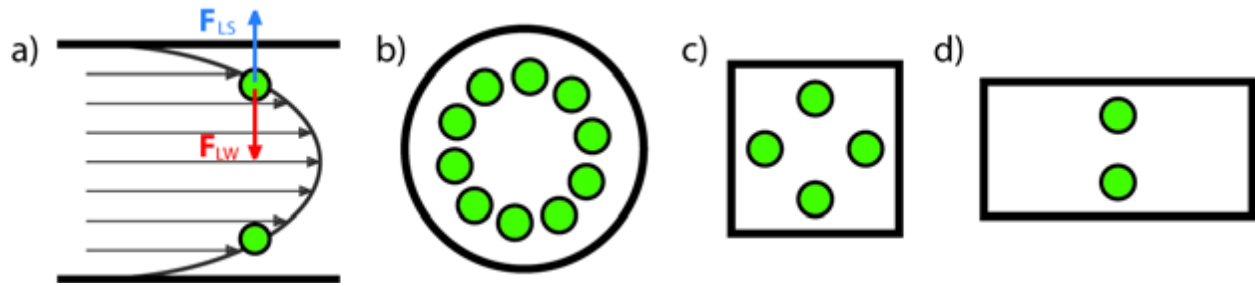


Figure 4.2: Particle experiencing inertial focusing in a microchannel. (a) A particle experiencing the shear induced lift force (F_{LS}) and a wall induced lift force (F_{LW}). (b, c and d) : Pictorial representation of the cross-sectional equilibrium positions of particles flowing through different channel shapes: round, square and rectangular respectively (Taken from Jonas Hansson, 2012).

Dino Di Carlo had put forward simple equations for fluid flow in straight rectangular systems that can help in designing micro-chambers (Dino Di Carlo, Lab Chip, 2009) :

(1) Channel length (L_f) required to focus the particles to equilibrium positions:

$$L_f = (\pi * \mu * H^2) / (\rho * U_m * a^2 * f_L) \longrightarrow \text{Equation (II)}$$

Where,

f_L : Lift coefficient (0.02–0.05 for aspect ratios from 2 to 0.5)

H : channel width.

μ : fluid viscosity

ρ : density,

U_m : maximum channel velocity

a : particle diameter.

π : pi = 3.14

(2) Flow rate (Q) :

$$Q \approx (2 * \pi * \mu * W * H^3) / (3 * \rho * L * a^2 * f_L) \longrightarrow \text{Equation (III)}$$

Where,

a : particle diameter

H : channel dimension(in the direction of particle migration)

W : channel width in the perpendicular direction.

L : channel length.

μ : fluid viscosity

ρ : density,

f_L : Lift coefficient.

π : pi = 3.14

(3) Lift force (F_L) is directly proportional to the fourth power of the particle diameter.

A lift coefficient (C_L) has been introduced by Asmolov to show a complete relationship between the lift force and the variables upon which it is dependent (E. S. Asmolov, J. Fluid Mech., 1999):

$$F_L = C_L * G^2 * \rho * a^4 \longrightarrow \text{Equation (IV)}$$

Where,

F_L : Lift force

C_L : Lift coefficient.

G : shear rate

ρ : density

a : particle diameter

This equation implies that by increasing the shear rate, the lift force required for the particle to be brought into equilibrium position can be increased by the square of the increased shear. So, for a particle of a constant diameter, the flow length of the channel required for achieving equilibrium will be comparatively lesser for a device capable of a higher shear rate of flow.

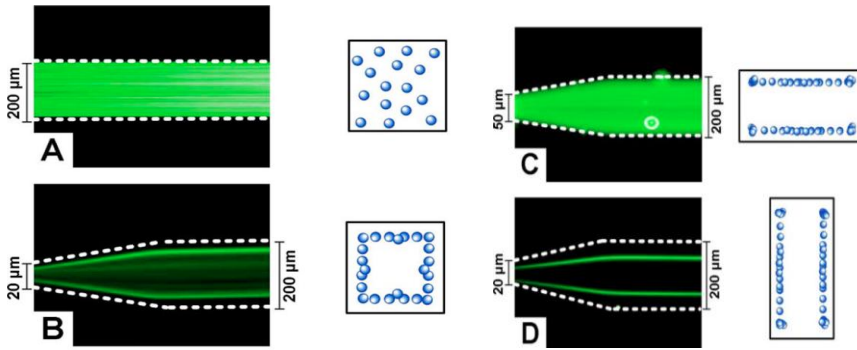


Figure 4.3: Representative image for focusing of particles in narrowest dimension, which is showing (a) inlets and outlets of (b) $20 \times 20 \mu\text{m}^2$, (c) $50 \times 20 \mu\text{m}^2$ and (d) $20 \times 50 \mu\text{m}^2$ microchannels. The ends at $20 \mu\text{m}$ are the narrowest dimension in the above design. Adjacent drawings show the approximate positioning of particles at equilibrium along the narrowest dimension's wall. (Taken from A.A.S Bhagt et al, Physics of fluids, 2008).

- (4) For rectangular microchannels, the narrowest channel dimension is the characteristic length, , typically denoted by channel width(w). Therefore, the lift force expression can also be given as (A.A.S Bhagt et al, Physics of fluids,2008):

$$F_L = (4 * \rho * U_f^2 * C_L * a_p^4) / w^2 \longrightarrow \text{Equation (V)}$$

Where,

F_L : Lift force

C_L : Lift coefficient

ρ : density

a_p : particle diameter

U_f : average flow velocity

w : width of the narrowest dimension.

(5) Upon applying the Stokes' law ($F_L=3*\pi*\mu*a_p*U_L$) into Equation (V) the following equation for particle lateral migration velocity (U_L) can be derived(A.A.S Bhagt et al, Physics of fluids,2008) :

$$U_L = F_L / (3 * \pi * \mu * a_p)$$

$$= 4 * \rho * U_f^2 * C_L * a_p^3 / (3 * \pi * \mu * w^2) \longrightarrow \boxed{\text{Equation (VI)}}$$

Where,

C_L : Lift coefficient

ρ : density

a_p : particle diameter

U_f : average flow velocity

w : width of the narrowest dimension

μ : fluid viscosity

π : pi = 3.14

(6) Thus for a particle's complete migration to it's equilibrium position, the required microchannel length(L) can be calculated from the following equation(A.A.S Bhagt et al, Physics of fluids,2008):

$$L = (U_{\max} * L_p) / U_L \longrightarrow \boxed{\text{Equation (VII)}}$$

$$= (2 * U_f * L_p) / U_L \longrightarrow \boxed{\text{Equation (VIII)}}$$

$$= (3 * \pi * \mu * w^2 * L_p) / (2 * \rho * U_f * C_L * a_p^3) \longrightarrow \boxed{\text{Equation (IX)}}$$

Where,

w : width of the narrowest dimension

μ : fluid viscosity

ρ :density

C_L : Lift coefficient

L_p : maximum required migration distance

U_{\max} : maximum flow velocity

U_f : average flow velocity

a_p : particle diameter

U_L : lateral migration velocity.

π : pi = 3.14

Therefore, from equation number IX, it can be concluded that lesser the width of the outlet focusing micro-channel (that is the channel of narrowest dimension) lesser will be the length of the preceding micro-channel required for bringing the particles of diameter 'a' to their equilibrium positions.

4.3 Diffusive mixing:

In microfluidics' applications, most of the flow deals with Reynolds number less than one. So the mixing phenomenon at the micron level is different than the macroscopic fluid dynamics. According to Aref (Aref, H. J Fluid Mech. 1984) diffusive mixing takes place in micro fluidics, in that both stirring and diffusion may occur simultaneously. Stirring is defined as the advection of the particles meant to be mixed without undergoing diffusion. Diffusion follows Fick's law, which states that the diffusion of one species through the interface is proportional to the concentration gradient of the species. In micro-fluidics the diffusive mixing is governed by the following equation:

$$x = \sqrt{(2D\tau)} \longrightarrow \boxed{\text{Equation (X)}}$$

Where,

$$x = \text{Diffusionlength}$$

$$D = \text{Diffusionconstant}$$

$$\tau = \text{Diffusionrate}$$

While designing the fourth device in this project (Chapter 7), numerous curves were made in path of liquid flow in order to produce secondary flow currents. It is expected that these curves will contribute to the generation of a small amount of turbulence and also result in an increase in the interfacial area for mixing. Therefore, the concepts listed above led to a better understanding of the flow phenomenon in microfluidic devices, and helped us design specific features to assist in diffusive mixing of the fluids in the devices (Dino Di Carlo, Lab Chip, 2009).

Chapter 5. FABRICATION METHODS FOR MICROFLUIDIC DEVICES

Microfluidic devices are usually fabricated by micro-moulding methods (Duffy DC, et al, Chem 1998, McDonald JC, et al 2002). Typically, these consist of two independent steps involving photolithography on a hard substrate, followed by replication of a pattern in an elastomeric material using “soft lithography”.

5.1. Photolithography

Firstly, a master mould of silicon, containing a photoresist pattern which represents the channel design, is fabricated by photolithography. Photolithography utilises a spin coater to create a thin film of photoresist and a appropriate UV lamp to photo cross-link the liquid resist into a solid layer. This layer is exposed by a photomask that projects the desired pattern on the photoresist, similar to the negative image of a photograph. Upon exposure with UV light, only the pattern exposed by the photo mask gets developed, leaving behind a micron scaled pattern for the master mould on a silicon substrate.

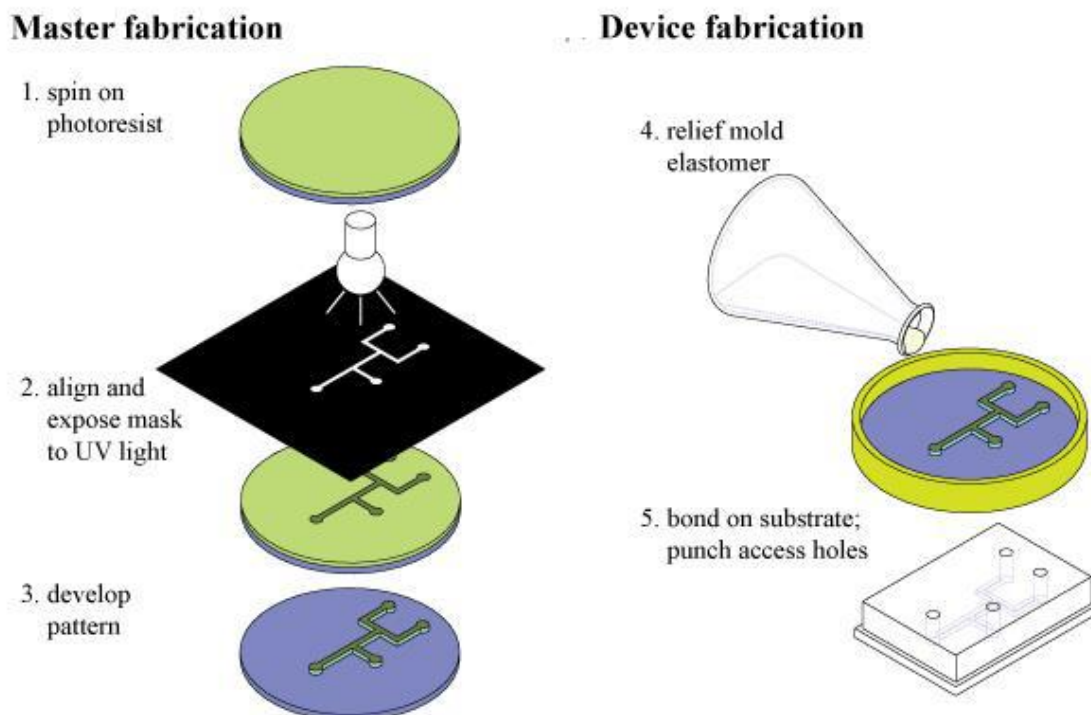


Figure 5.1 : Fabrication procedure for a single layer microfluidic device.(Taken from The European Physical Journal Special Topics, Probing single cells using flow in microfluidic devices, 2012, 87, Qi, D., Hoelzle, D.J, et al.

5.2. Soft Lithography

Next, a liquid elastomer like Poly Dimethyl Siloxane (PDMS) and a curing agent are mixed and poured onto the master mould and cured at 60 °C for 2 h. The disassembly of the mould and PDMS replica is performed and the resulting microfluidic device is then cut according to the dimension. Appropriate holes may then be drilled into the device through needles for fluid inlet and outlet. For sealing of the full microfluidic device, plasma treatment is given to the PDMS microfluidic device and glass cover slip for 30 s. The cover-slip and PDMS device are then brought into contact with each other so that a covalent bond forms between them and a leak-proof seal is generated.

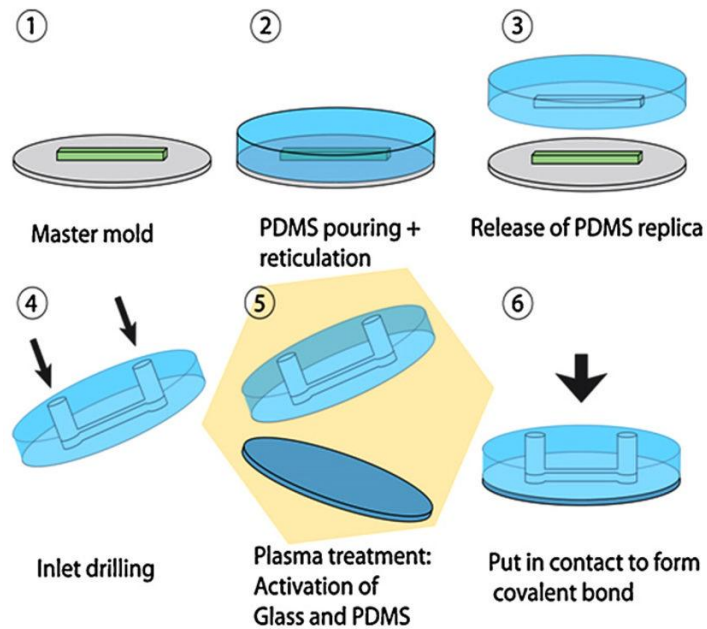


Figure 5.2: Pictorial representation of Soft lithography process. (Taken from Guilhem Velasco-Casquillas et al, 2010).

Chapter 6. INITIAL PROTOTYPING

6.1. Design of a basic microfluidic pattern and analysis of the fluid flow in it.

Rationale: Since photolithography is a very expensive and time-consuming fabrication process, initial prototyping was done using micron-scaled consumables as described below. Molten agar was used as a soft elastomeric agent instead of PDMS, both to conserve prototyping costs and also to evaluate its use for ensuring viability of isolated bacteria.

Materials:

1. 0.15x22 mm circular cover glass.
2. 0.12x13 mm circular cover glass.
3. 0.5x20 mm glass capillaries.
4. 22x60 mm cover glass.
5. Square and circular petri dishes.
6. LB Agar.

Design Calculations:

1. Volume of the three smaller cylindrical chambers = $\pi r^2 h = 3.14 * 6.5 * 6.5 * 0.12 = 15.92 \text{ mm}^3 \sim 16 \text{ }\mu\text{l}$.
2. Volume of the cylindrical channels = $\pi r^2 h = 3.14 * 0.25 * 0.25 * 20 = 3.925 \text{ mm}^3 \sim 4 \text{ }\mu\text{l}$.
3. Volume of the central cylindrical chamber = $\pi r^2 h = 3.14 * 11 * 11 * 0.15 = 56.99 \text{ mm}^3 \sim 57 \text{ }\mu\text{l}$.

Procedure:

1. A preliminary design of a simple microfluidic mixing device was created as shown in Figure 6.1 A below.
2. The 0.12x13 mm circular cover slips were used to mold inlets for the liquid sample (three in number).
3. They were connected to the central mixing bay area (made by the 22m diameter circular cover glass) by equally cut capillary tubes at an angle of 45 degrees from each of the smaller cover glasses.

4. A rectangular cover glass was used to make the waste collecting area that was connected to the central cover glass using an equally cut capillary tube.
5. The above design was pasted onto the square petri dish and upon it molten agar was poured to cast the pattern onto the gel.
6. Three different food dyes were used to make three liquid samples that were further allowed to flow from the three different chambers into the central area and then they were collected into the rectangular waste chamber.

OBSERVATIONS:

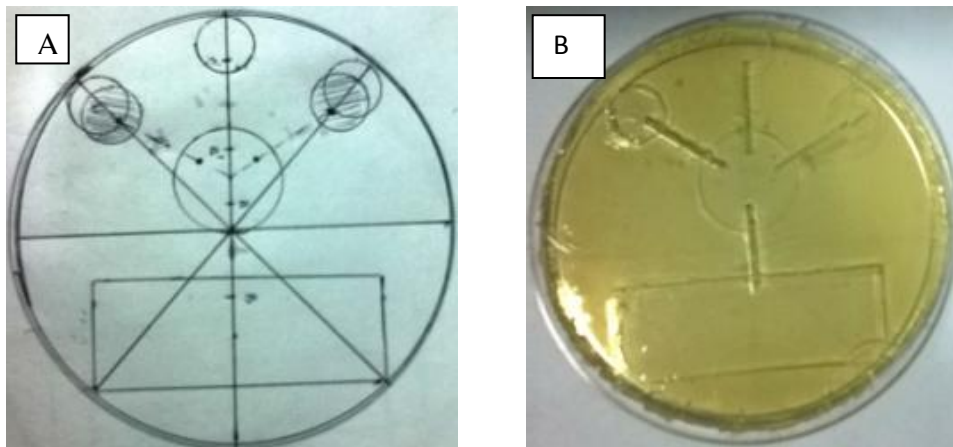


Figure 6.1: Designing of Micro pattern using slides and cover slips. (A) Design on white sheet of paper. (B) Design on agar containing petri dish.

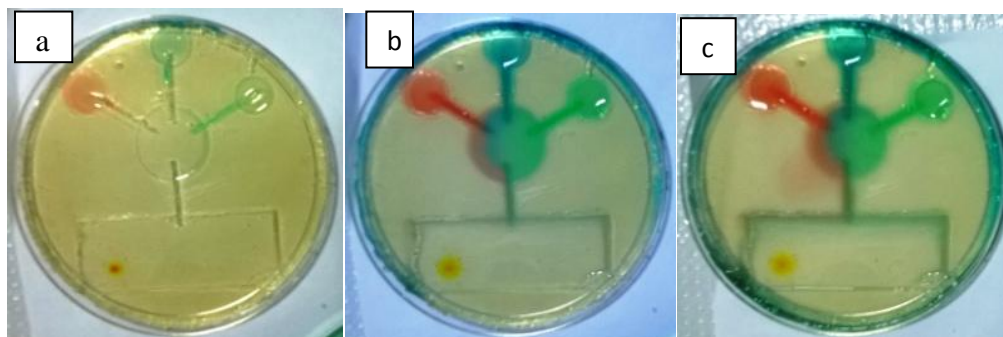


Figure 6.2: Flow of coloured dyes in micro channels. (a) Initial flow at 50 μL in each of the three smaller circular chambers. (b) Flow at 250 μL . (c) Flow at 500 μL .

Result and Discussion:

Upon injection of 50 μl of the fluid into each of the three smaller cylindrical chambers, the liquid started to flow into the device but it stopped before reaching to the central chamber. By combining up of the volumes of the three smaller cylindrical chambers and the three channels, the volume comes to 60 μl . However, even though the total volume injected was 150 μl , the flow stopped at the opening of the central chamber. This might have happened due to the surface tension of the LB agar gel.

At 250 μl of injection, well-defined laminar flow of each of the three fluids were observed in the central chamber and also the liquid started to flow towards the rectangular chamber. Since there was no natural turbulence or any specific features to induce it, mixing of the three injected fluids was not seen.

At 500 μl of injection, an overflow was observed in the central chamber. This might have happened due to blockage in the channels leading to the rectangular waste chamber or due to faster injection rate of the fluids as compared to its flow rate within the channels. Also it can be observed in Figure 6.2c that there was flow of coloured liquid outside the prototype device, potentially because of the improper casting of the device.

Incorporating the lessons learnt from this experiment in the final device, the final design may be improved by having deeper chambers, smooth channels, delayed fluid injection timing and improved casting of the device from the mould.

Conclusion:

A successful preliminary prototype for evaluating microfluidic flow patterns was devised and a beautiful laminar flow of the fluid was observed. However, in order to mix the solution in the central chamber, some additional patterns need to be designed such that small eddies or vortices are generated to create a turbulent flow. This would aid in mixing the drug solutions in the central chamber.

Chapter 7. COMPUTER AIDED DESIGN

7.1 SOLID MODELING:

The 2015 version of SolidWorks™ software has been used to make the 3D solid models of the designs for the microfluidic devices. Briefly, a basic 2D sketch of the features of the design was created on a pre-selected base plane, typically the X-Y plane. The features of the sketch were then extruded in the third (Z) direction to construct the 3D solid model. Adding extruded cut and shell options in the software to make inlet, outlet and other cavities in the design further refined the 3D model. Filleting was performed at sharp edges before making extruded cuts. Mirror option both for the 2D sketches and 3D features were used to construct identical and symmetric structures in the design by selecting the appropriate plane at a desired distance with the help of centerline. Some of the designs were made in parts and were then assembled together to give the final assembly of the device. A detailed description of each of the four designs created is given below. Dimensions listed on the sketches and solid models are typically in microns.

Design No. 1:

The purpose of this design is to create a basic micro-channel device that may be used to study the flow conditions and device parameters required for single cell isolation. This is the simplest design, consisting of a series of parallel channels (Figure 7.1 A) with an aspect ratio of 1.1 (i.e. width of 50 μm and height of 45 μm). These channels are connected at right angles to two parallel trenches on either end of the channel, which may be interchangeably used as common inlet and outlet ports (Figure 7.1 B). In this basic design, a uniform height (50 μm) is maintained for all features to establish conditions for basic laminar flow and to minimize turbulence or flow restrictions.

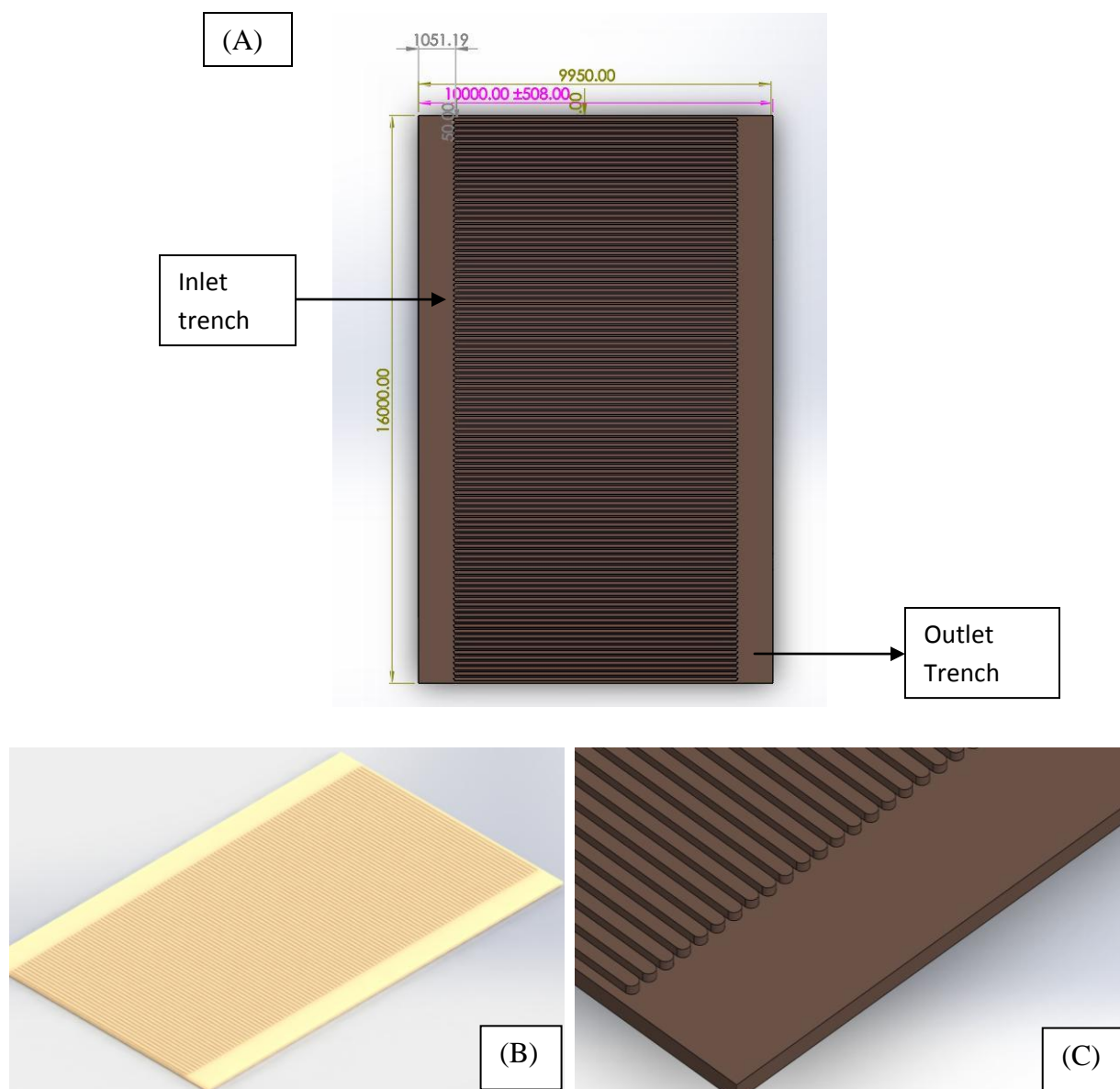


Figure 7.1: (A) 2D Sketch of the basic channel design. (B) 3D Isometric view of solid model generated after rendering in Solid Works™ (C) Zoomed in image of first design showing the channels and outlet chamber.

Design No.2:

The purpose of this design is to establish conditions for maintaining the viability of the bacterial for at least 2 generations and potentially up to 5 generation. This would allow us to study the morphological changes in the isolated bacteria as they were dividing. In order to allow for additional space in the channels to accommodate the dividing bacteria, the aspect ratio of the individual channels was increased to 2.2 (i.e. width of 100 μ m and height of 45 μ m). It was also realized that maintaining flow of media for a sustained period of time (equivalent to or greater than the time for cell division) would result in a fairly large volume of bacterial media being pumped in. This would imply that a greater volume of waste media would be generated. Hence, the dimensions of the inlet and outlet chambers were modified to accommodate the larger volumes of fluid that this design was expected to encounter.

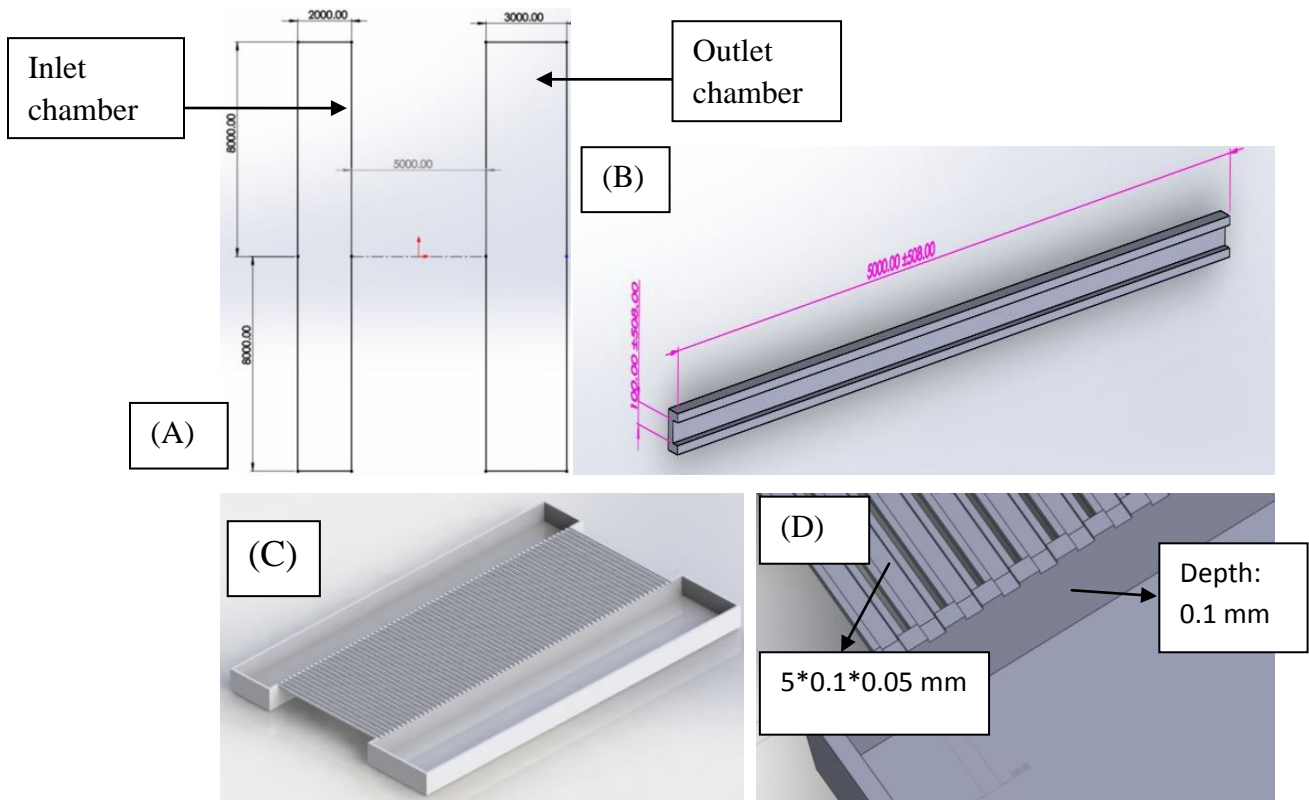


Figure 7.2 : (A) 2D sketches of the modified inlet and outlet chambers. (B) Isometric (3D) detailed view of a interconnecting channel as an independent part. (C) 3D isometric view of the complete assembled device generated after rendering in Solid Works™. (D) Zoomed in view of the channels connected to the outlet chamber.

Design No.3:

The purpose of this design is to optimize the flow conditions required to isolate a stained single bacterium into each individual channel. For this purpose, a series of tapering inlets were appended to the inlet chamber. As seen in Figure 7.3 (A&B), this helps firstly in aligning the bacterium to their equilibrium positions along the walls of the narrowest dimension, before being isolated in the central chamber. (Ali Asgar S. Bhagat et al. *Physics of Fluids* 20, 101702, 2008).

Further, it is well known that fluid flow takes the path of least resistance. Since the dimensions of the input and output chambers are substantially larger than that of the central channels, the fluid is likely to resist flow into and across the channels and simply flow right along the sides. Hence, in order to optimize the flow into the central channels, a series of semi-circular boss elements were aligned at the inlet and outlet ends of each individual central channel as shown in Figure 7.3 (C &D). These boss features provide additional resistance to the flow along the inlet and outlet chamber and serve as strategic obstructions that help focus the flow into the central channel.

The modified design allows the distribution of the monolithic central channels from the previous two designs into a series of smaller sub-units, each of which has a sub-assembly of parallel channels for bacterial isolation. This allows for the study of multiple devices in parallel, while potentially varying the local flow and study conditions for each individual sub-device. As a result, this design allows us optimized isolation as well as multiplexing of independently variable study conditions in a single integrated device. For example, using this design, we can either introduce multiple clonal populations of the same bacterial strain in each independent sub-device, or then modulate the local environment by inputs of multiple variants of media, antibiotics or other environmental challenges to each unit. The complete assembly of the modified inlet and outlets with the integration of multiple sub-devices is shown in Figure 7.4.

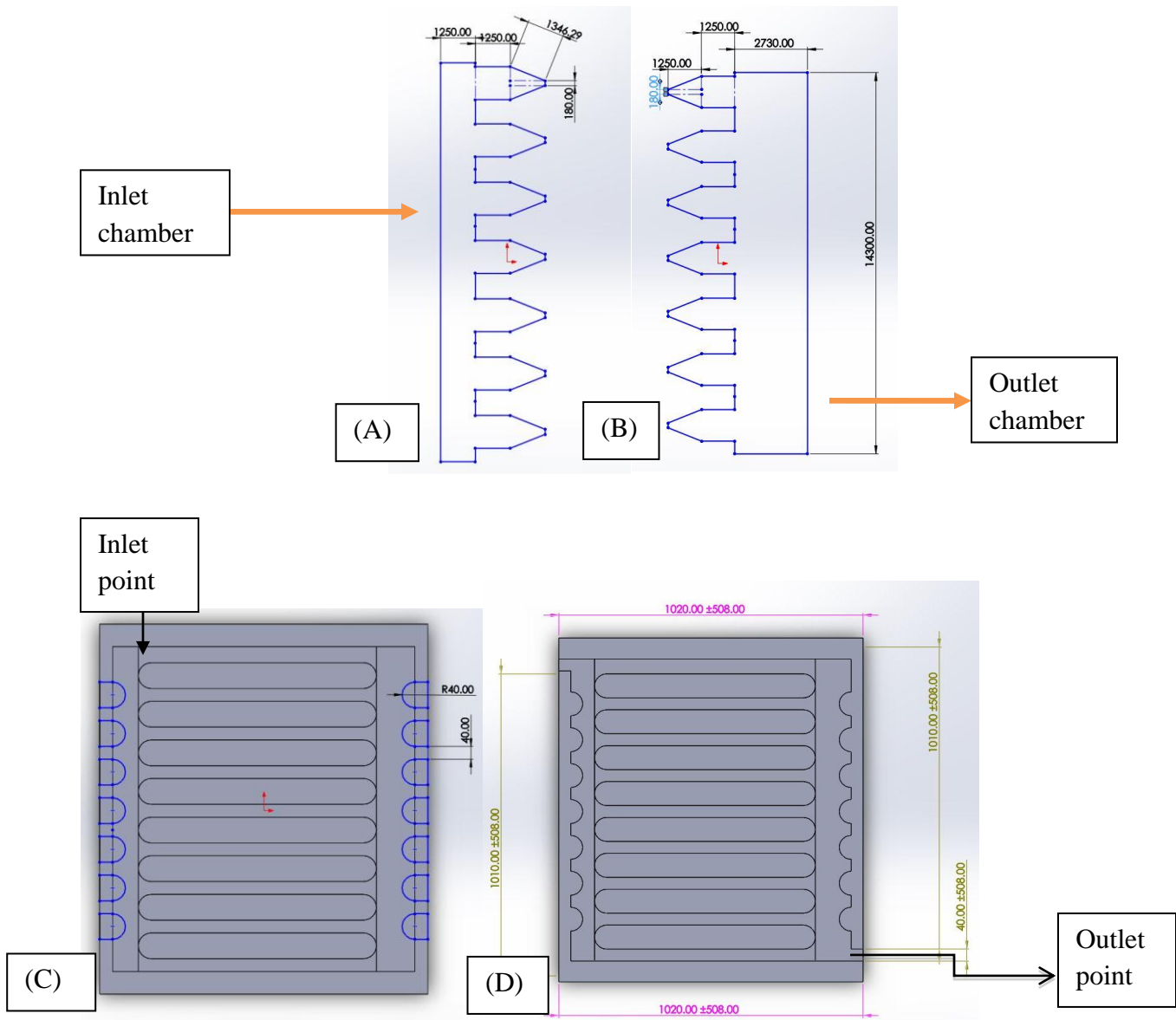


Figure 7.3: (A and B) 2D Sketches of the modified inlet and outlet chambers with tapered ends for flow focusing and streamlining bacteria for isolation. (C and D) Sketches of the modified central chamber, with flow focusing boss structures at the channel inlet and outlets.

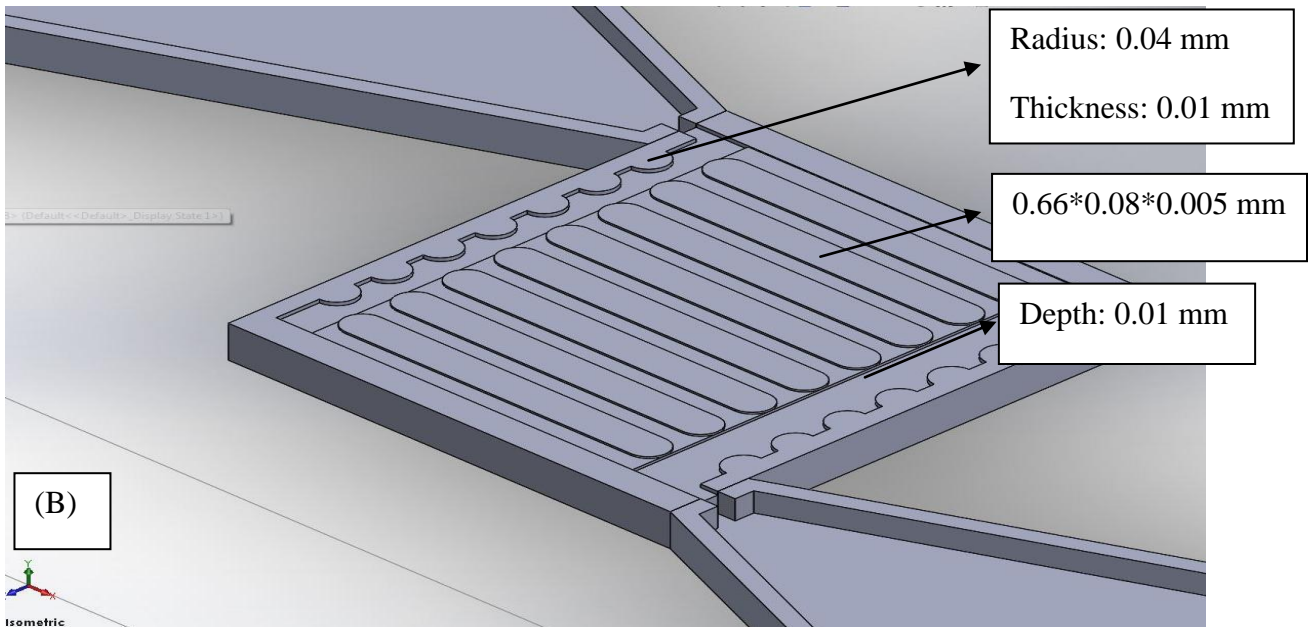
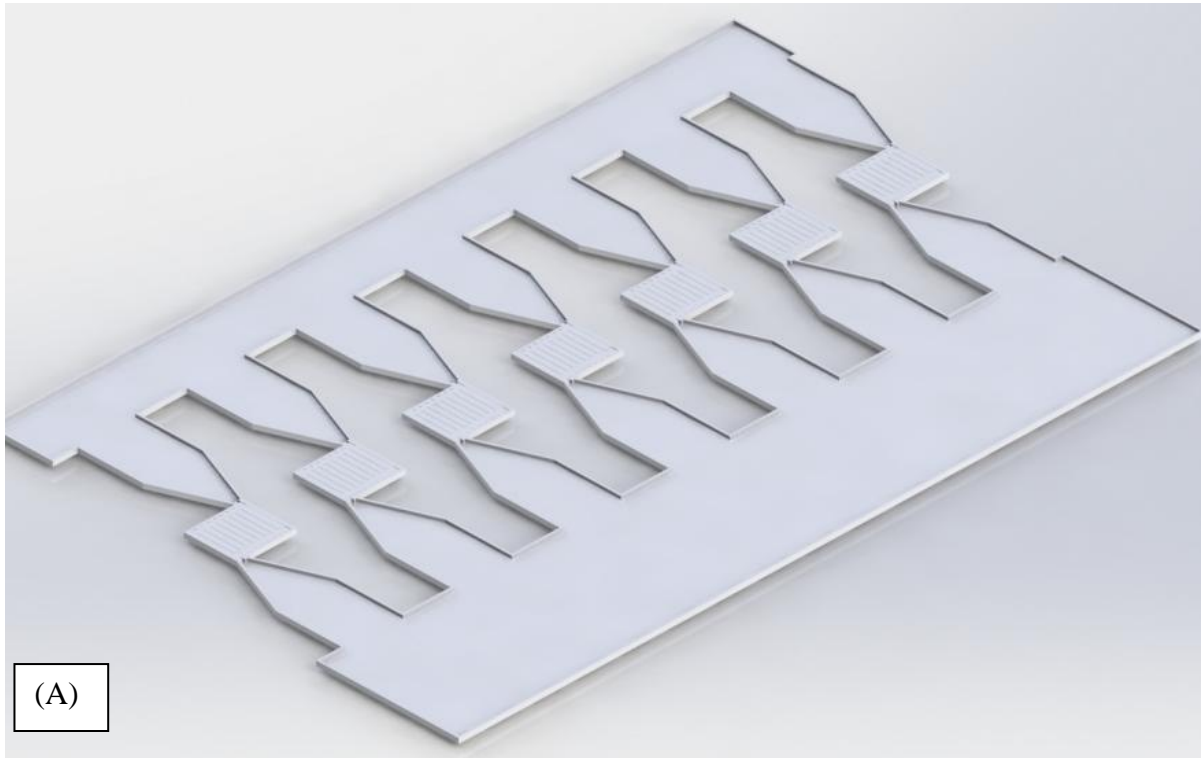


Figure 7.4: (A) The complete assembled design no.3 in isometric 3D view generated after rendering.(B) Zoomed in view of the third design showing the dimensions of the central chamber.

Design No.4:

This design is intended to isolate the bacteria in the central chambers and to simultaneously perform dynamic mixing of various input fluids, such as drug solutions, in the device itself while the fluid is moving through the curved channels (Dino Di Carlo, Lab Chip, 2009). This will allow the evaluation of dynamic flow of various drugs on the isolated bacteria and to establish sensitivity or resistance.

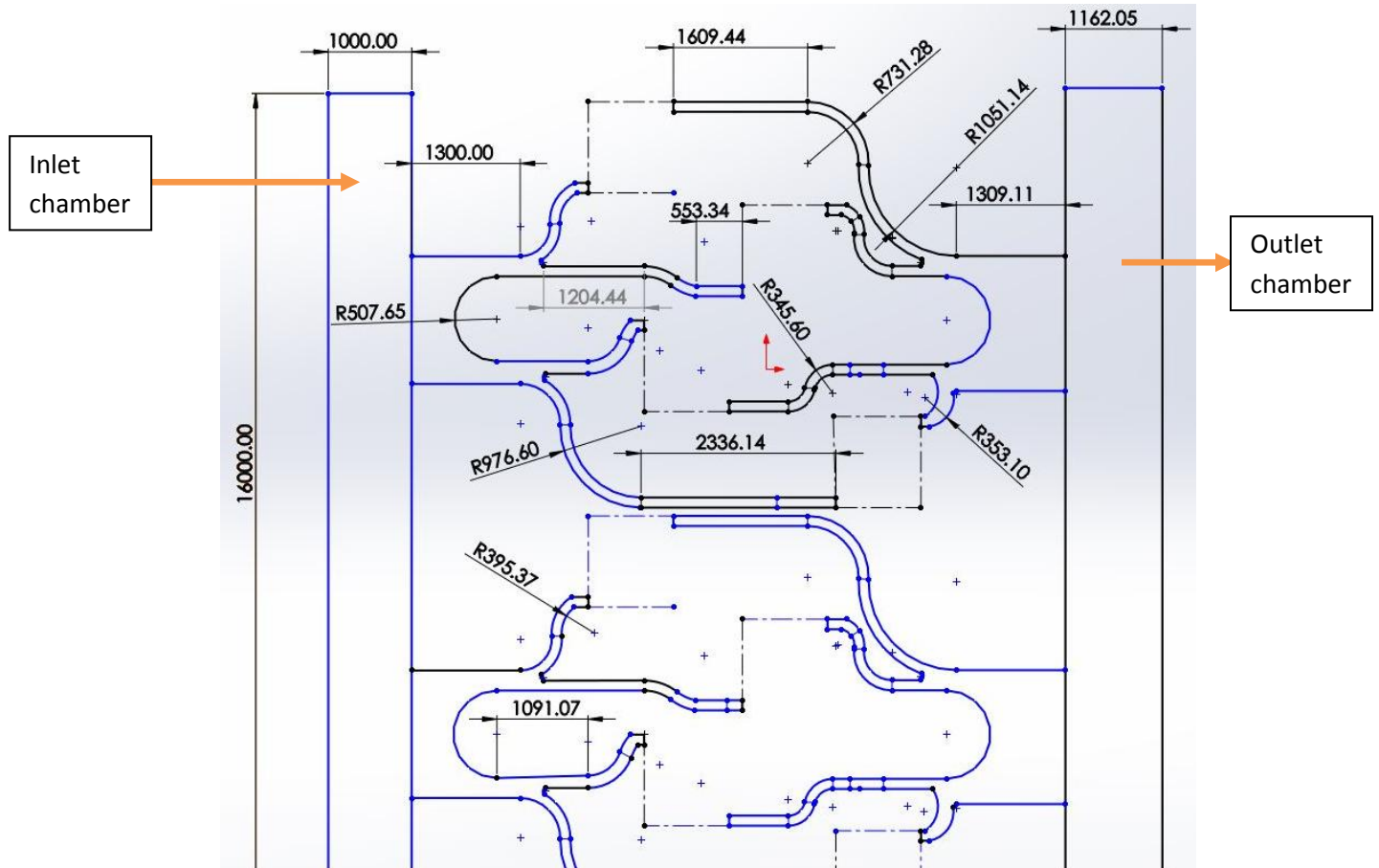


Figure 7.5: 2D sketch of inlet, outlet chambers and connectors to the central chamber to enable dynamic mixing of input fluids. (All dimension shown here are in micron-meter).

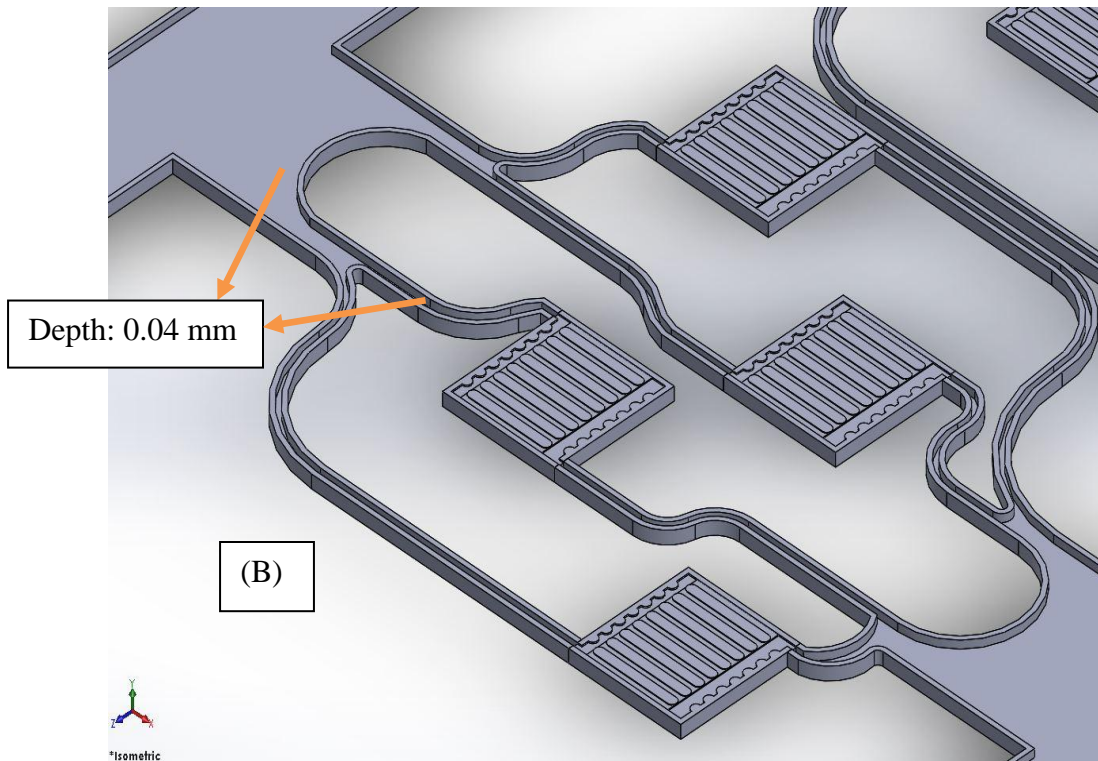
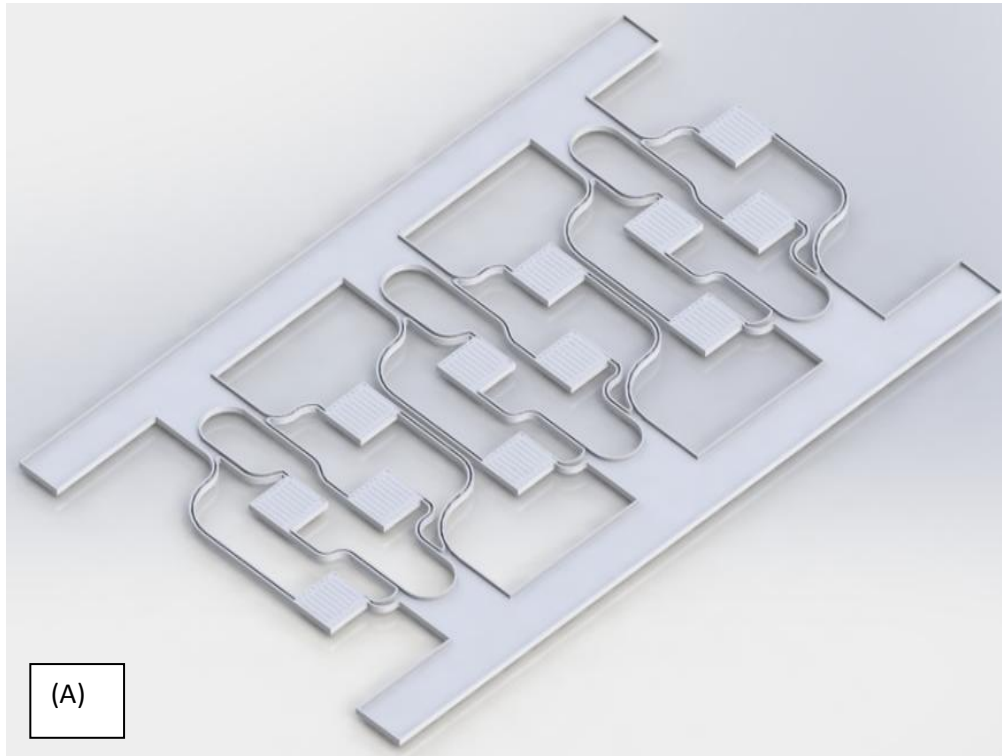


Figure 7.6: (A) Complete assembly (3D Isometric view) of fourth design after rendering in Solid Works™. (B) Zoomed in image showing the depth of the inlet and outlet ports and channels in the fourth design.

7.2 AUTOCAD DESIGNS:

The photo mask printer requires an input of files in the “*.gerber” file format for the printing of the photo mask. Since files generated in the SolidWorks™ software could not be converted into the required format, the designs had to be remade in AUTOCAD™ software, from which files were easily convertible.

During this conversion process, some changes were made in the original solid models in AUOTCAD™, including a change in the features of some designs which were difficult to get manually aligned. The modified designs in the appropriate file format for photomask printing are listed below.

Design No.1:

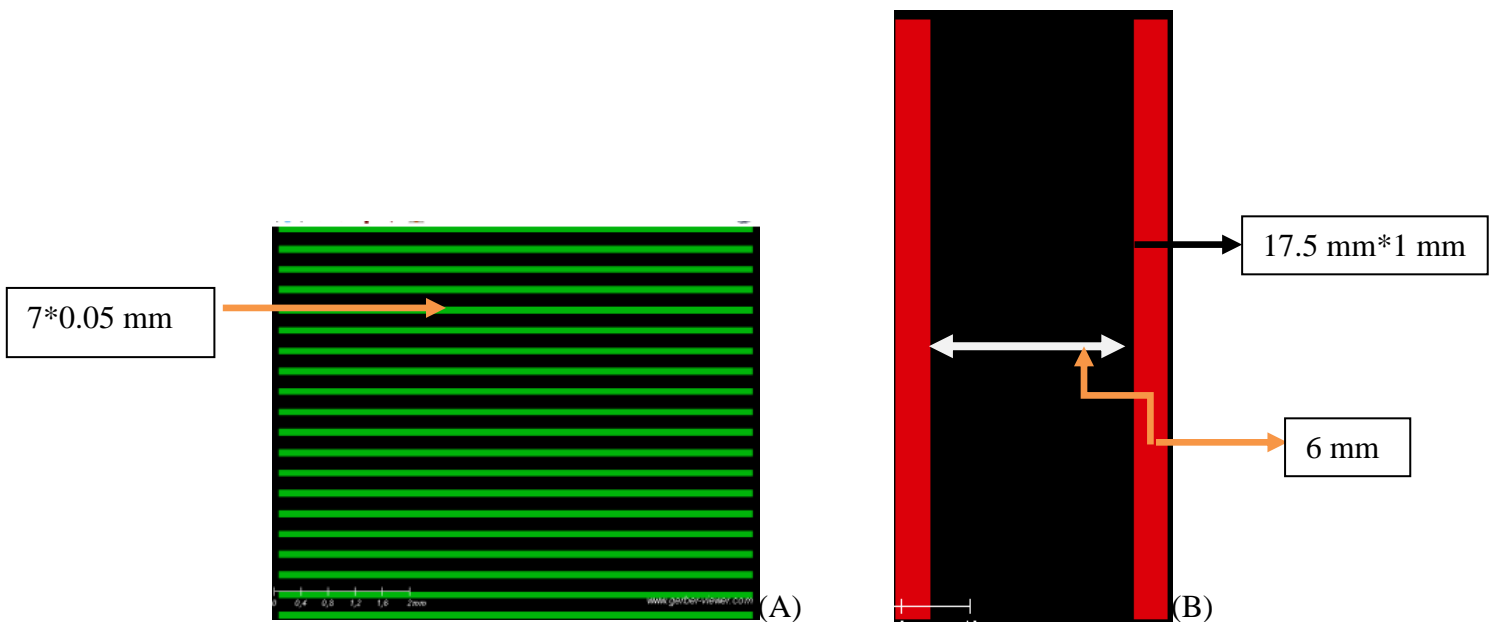


Figure 7.7: (A) High resolution annotated image of central channel. (B) The inlet and outlet chambers of approximately 125 micro-meter height.

Design No.2:

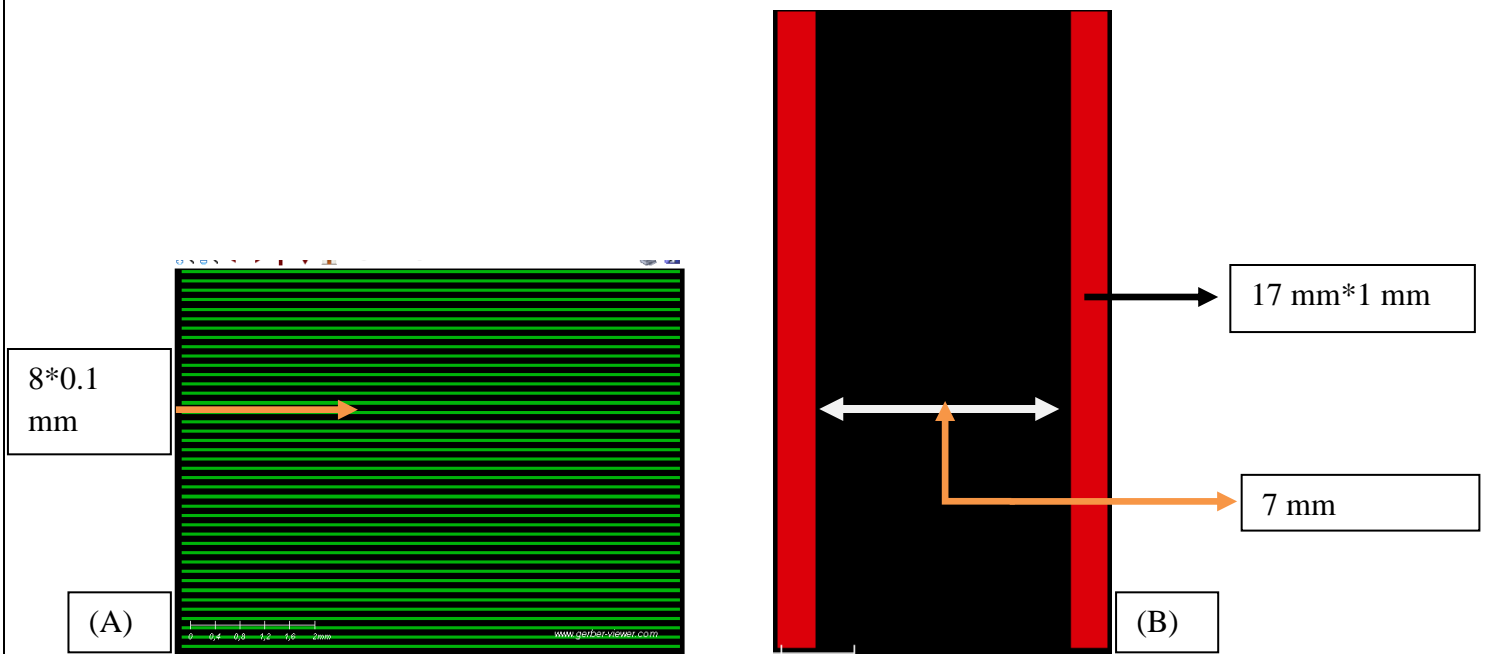


Figure 7.8: Annotated images of AUTOCAD designs in gerber file viewer of second design. (A) The zoomed in annotated image of central channel of 45 micro-meter width. (B) Layout of the inlet and outlet chambers of 125 micro-meter height.

Design No.3:

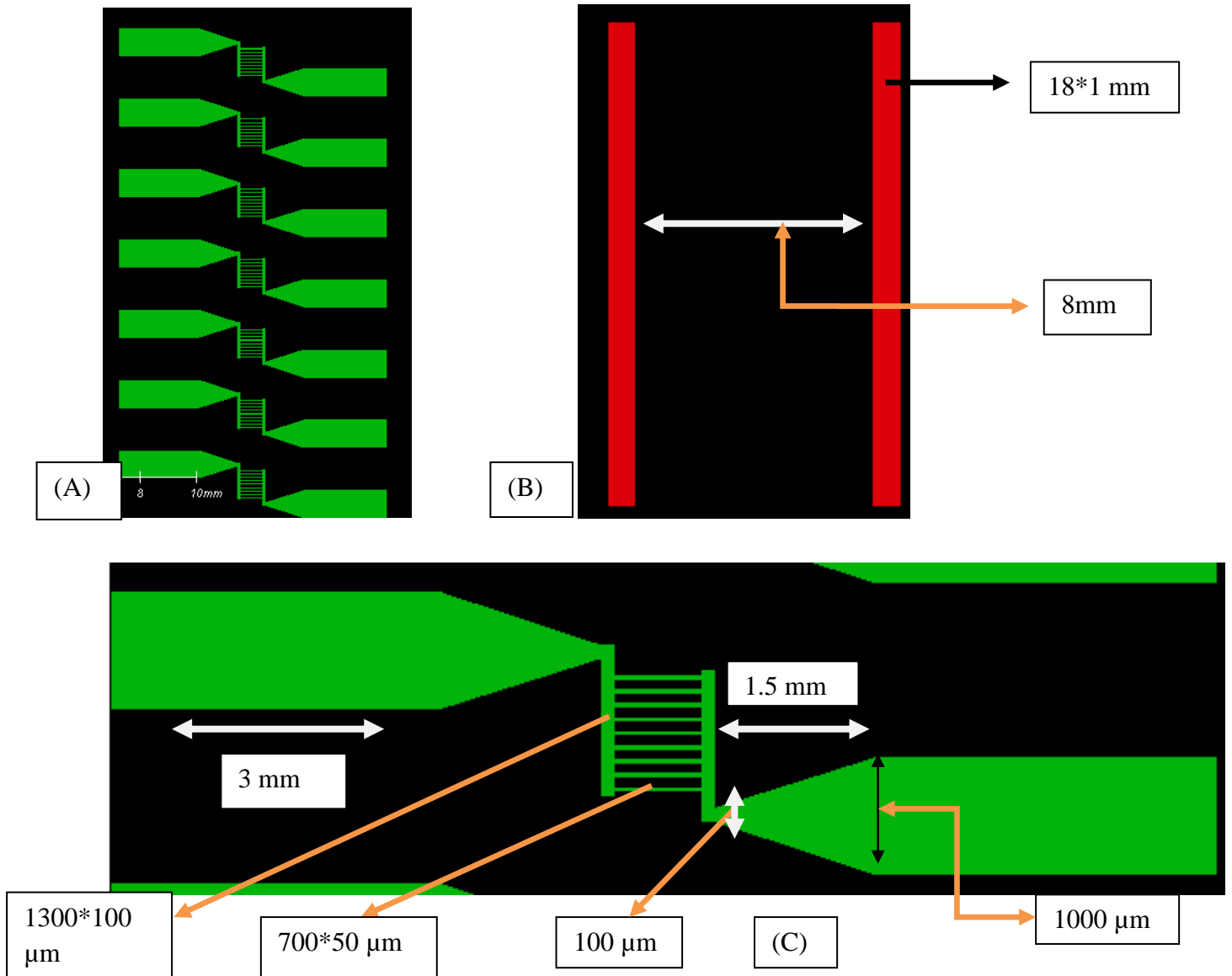


Figure 7.9: Images of AUTOCAD designs in gerber file viewer of third design. (A) The central design of 45 micro-meter thickness.(B)The inlet and outlet chambers of approximately 125 micro-meter height.(C) The zoomed in annotated image of central channel.

Design No.4:

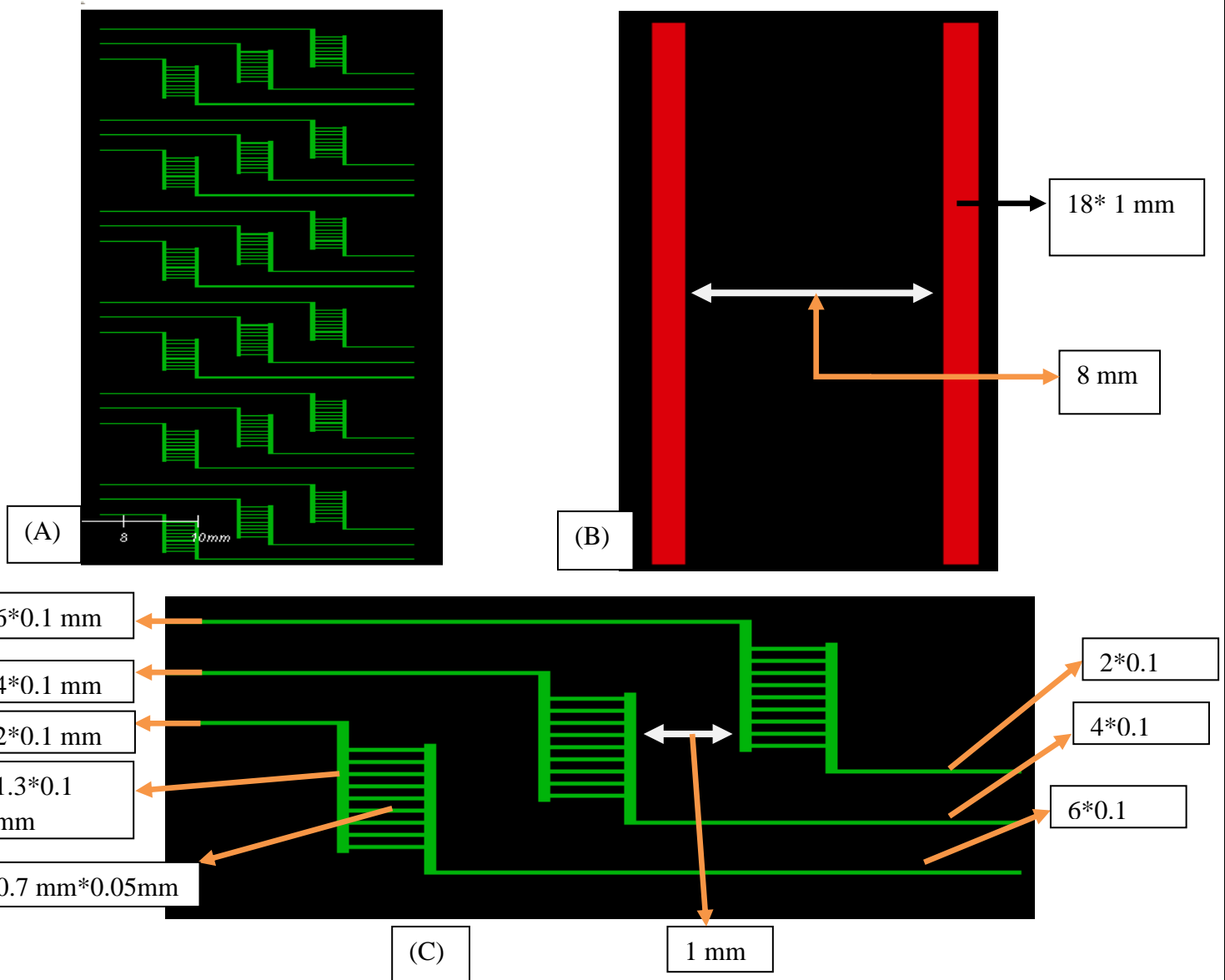


Figure 7.10: Images of AUTOCAD designs in gerber file viewer of fourth design. (A) The central design of 45 micro-meter thickness.(B)The inlet and outlet chambers of approximately 125 micro-meter height.(C) The zoomed in annotated image of central channel.

Chapter 8. MATERIALS AND METHODS

8.1 Preparation of Bacterial culture:

(A) Culture of *Mycobacterium Smegmatis* (*M.Smeg*):

Materials:

Autoclaved Complete 7H9 medium: Dissolve 4.7 g Middlebrook 7H9 broth base in 900 mL de-ionized water. Add 10 mL of 50 % glycerol, 2 mL of 10 % Tyloxapol), Glycerol: 50 % (v/v). Tween-80: 10 % (w/v). 50 mL falcons, 5 µm filter unit, 0.22 µm filter unit, 1 mL and 10 ml syringes.

- (I) 10 mL of autoclaved complete 7H9 medium was inoculated in a 50 mL falcon with 100 µL of glycerol stock of mCherry strain and wild type *M.Smeg*.
- (II) To the mcherry strain 50 µg/ml of hygromycin was added.
- (III) The culture was kept in shaking incubator for 12 hours at 37°C, till it reached an O.D. of 0.6.
- (IV) The bacteria was harvested in 1ml Eppendorf tubes by centrifugation at 4000 rpm for five minutes at 4°C.
- (V) The bacterial pellet was re-suspended in 500 µL of pre-warmed complete 7H9 media.
- (VI) The concentrated bacteria was taken in a 1 mL syringe and made to pass through a 5 µm filter to ensure that bacterial clumps were removed.

(B) Culture of *Escherichia coli*:

Materials:

LB agar, Autoclave, 50 mL falcons, 5 µm filter unit, 0.22 µm filter unit, 1 mL and 10 ml syringes.

Procedure:

- (I) To the 10 mL of LB broth, 100 µL of the glycerol stock of wild type *E. coli* was added in a 50 mL falcon.
- (II) The culture was kept in a shaking incubator at 37°C for 20 minutes.
- (III) After 20 minutes, the O.D. of the culture was measured to ensure the bacteria was viable and dividing.
- (IV) Depending upon the O.D. it was further re-cultured to get an O.D. of 0.2-0.4

- (V) The culture was taken into two 1 mL Eppendorf tubes and centrifuged at 4000 rpm for 5 minutes at 4°C.
- (VI) The bacterial pellet was re-suspended in LB broth or PBS (pH 7.4) as per further requirement.

Note:

1. mCherry is an extra-chromosomal plasmid bearing mycobacterium which shows constitutive expression of pink coloured protein that is used for this experiment to confirm that the bacteria which is being isolated and visualized is the mycobacterium and second that upon usage of Confocal microscopy, cell wall degradation and plasmid degradation during cell death can be studied.
2. All the reagents which could not be autoclaved were filter sterilised and those instruments which could not be autoclaved were UV sterilised.

8.2 FITC Staining of Bacteria for Live Cell Imaging:

Principle: In order to visualize the bacteria isolated in the microfluidic device, it was necessary to stain them with a fluorescent dye. This is necessary because bright-field imaging does not provide adequate resolution for identifying morphological changes at the single cell level, as is required for our purpose. FITC is a well-known fluorescent dye in which the isothiocyanate group reacts with amino terminal and primary amines in proteins present on the cell membranes.

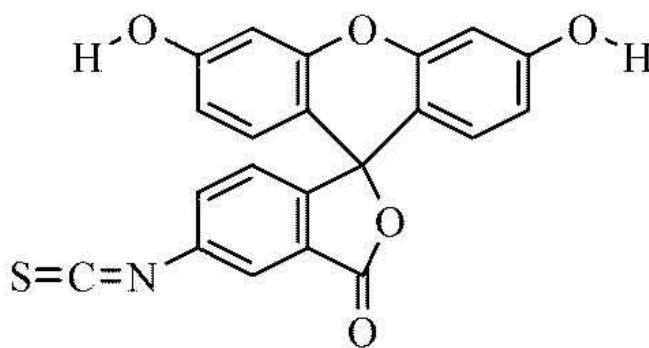


Figure 8.1: FITC molecular structure.

Materials:

FITC, bacterial culture (wild type), sodium bicarbonate, Double –ionised water (DI), PBS buffer (pH 7.4), 0.22 micron- meter filter, 1mL and 10 mL syringe, 7H9 complete media.

NOTE: Solutions were freshly prepared for each assay.

Procedure:

A. Preparation of stock solutions:

1. 10 mL of 0.1 M sodium bicarbonate buffer, pH 9.0
 - a. 84 mg of sodium bicarbonate was added to 10 mL of DI water.
 - b. pH was adjusted to 9.0 with sodium hydroxide
 - c. Solution was filter sterilized using syringe filter.
2. 0.1 mg/ml FITC solution was made in PBS buffer (pH 7.4).

B. Preparation of FITC-labelled bacteria

1. Bacterial cells were harvested by centrifugation at 4500 g and 4°C for 5 min.
2. The bacterial cells were re-suspended in 1 ml of 0.1 M sodium bicarbonate buffer. (The optical density was measured at 600 nm from a 1:100 dilution of cell suspension in sodium bicarbonate. The cells were diluted to 10^{10} cells/mL in a total of 1 mL sodium bicarbonate).
3. 20µl of FITC stock solution was added to cell suspension and immediately vortex. The cells were incubated in the dark with end-over-end rotation for 45 minutes at room temp.
4. The cells were washed four times with PBS to remove unbound dye and re-suspend in 1 mL of complete pre-warmed 7H9 medium. The optical density was measured at 600 nm from a 1:100 dilution and the cells were re-suspended in 7H9 media.

8.3 Agarose-pad Microscopy:

Aim: This experiment has been performed to learn to image bacterium at a high resolution using a fluorescent microscope.

Materials: 1.5% agarose (Low melting point), Circular cover slips, forceps, 7H9 media, petridish, scalpel, microbial hood, Olympus IX83FC Inverted Fluorescent microscope.

Procedure:

1. Agarose pads were made by pouring the agarose and 7H9 complete medium (1:1, v/v) upon a circular cover slip placed in a petridish.
2. The agarose was then gently further covered by another cover slip of same dimension. This set up was allowed to cool and settle down for 20 minutes.
3. Then the upper cover slip is gently removed and with the help of forceps, and the agarose pad was flipped onto a glass slide and pasted by cello-tape.
4. On top of the freshly prepared pad, 2 μ L of the FITC-stained bacterial sample was smeared and allowed to be adsorbed on the pad
5. Inverted fluorescent microscopy was performed on the stained pads

8.4. Microfluidic Device Fabrication:

(I) Mould Preparation:

(a) Glass Slide Preparation:

1. The glass slides were cleaned by letting them put into a 5 mL solution of distilled water and liquid soap taken in 50 ml Falcon tubes, to remove the organic impurities present on the slides.
2. The above set up was kept in a microwave at normal heating for 20 minutes and then kept at room temperature for 35 minutes.
3. The soap solution was drained out and fresh distilled water was added into them and kept at room temperature for two hours.
4. After two hours again the water was drained out and fresh distilled water was put into those falcons, covered with aluminum foil and kept for overnight at room temperature.
5. The slides were taken out and dipped into Isopropanol and then in acetone and were further sonicated for 10 minutes at 30°C.

6. The slides were purged with dry Nitrogen gas to make it dry and ultra clean. If the slides were to be kept for further usage then they were stored in isopropanol.

(b) Spin Coating of Photoresist and Final Mould Formation

1. A dollop (half to one inch) of SU8(50) photoresist was poured onto the slide and then spun for 10 seconds at 500 rpm.

2. The spin speed was then further increased to 3000 rpm for 30m seconds.

3. Soft baking of the spin-coated slide was then performed at 65°C is performed for 5 to 10 minutes.

4. Manual alignment was used to align the photomask onto the SU8 and then UV exposure was done for 1 to 2 minutes.

5. After that the slide was baked at 95°C and a second layer of photoresist was coated upon it and spun at 1500 rpm for 30 seconds to obtain the second layer of design.

6. Again manual alignment was used to align the photomask onto the SU8 and then UV exposure was done for 1 to 2 minutes.

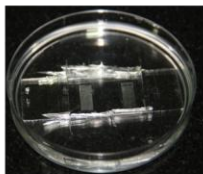
7. Further hard baking at 95°C was performed for 10 minutes to finalize the mold.

8. Chloroform was used to develop the mould and kept in an Aluminum foil.

9. Silanisation was performed by dropping 2-3 drops of trichlorosilane in a fume hood onto the master mould, so that the PDMS peeling off becomes easier.

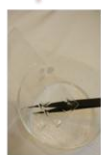
10. Now the mould was ready to be used after 12 hours of stabilization at room temperature.

Slide Preparation using Isopropanol/acetone treatment and sonication.



The Mould

Silanisation



Developing the design in chloroform



Spin coating of the SU-8(50) onto the slide.



Soft baking at 65°C for 10-15 minutes.



Manual aligning of the photo film containing the design onto the spin coated SU-8.



UV Cross-linking of the SU-8.



Baking at 95°C



Figure 8.2: Pictorial Representation of the mould preparation process.

(II) Soft Lithography Casting of Device from Moulds:

1. PDMS resin was taken in a ratio of 1:10 and mixed thoroughly and degassed in a desiccation chamber to remove the air bubbles.
2. The degassed PDMS mix was poured on to the mould and then kept at 70°C for 4 hours for the polymer to complete its polymerization.
3. Then with the help of scalpel the design etched on the PDMS was peeled off carefully.
4. Oxygen plasma bonding was performed to bind the PDMS device to the glass coverslip.

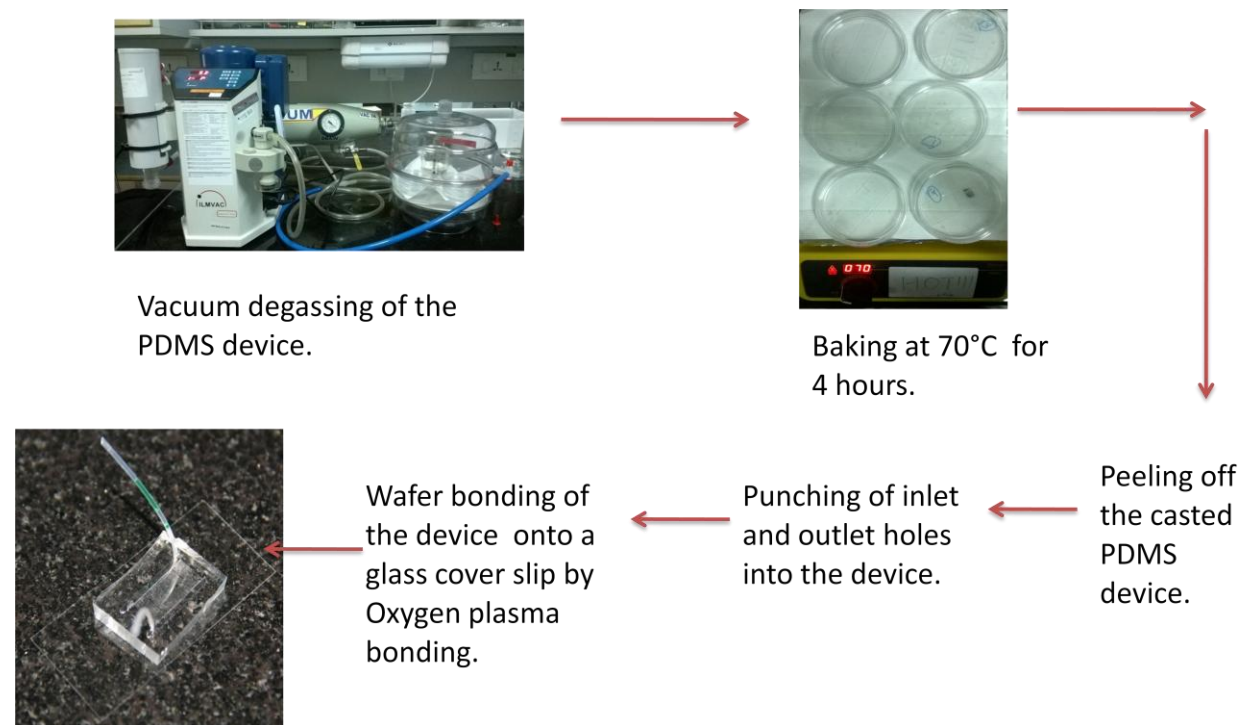


Figure 8.3: Pictorial representation of the PDMS casting process.

(III)Preparation of Microfluidic Devices for Bacterial Isolation and Imaging Experiments:

1. The inlet and outlet ports were connected with plastic tubing of 1 mm diameter.
2. The FITC stained bacterium and mCherry strain of strain of *M. Smeg* were taken into a 1 mL syringe and injected through the inlet ports at a rate of 25 μ L/min.
3. Fluorescent microscopy was performed at 4X, 10X, 20X and 40X using a Olympus IX83 FC instrument.
4. The FITC stained *E.coli* was treated with 25 and 50 μ g/ml of Kanamycin drug. The drug was taken into a 1mL syringe and injected through the device. Fluorescent microscopy was performed at 4X, 10X, 20X and 40X as before.

Chapter 9. RESULTS AND DISCUSSION

1. Agarose Pad Microscopy and FITC staining:

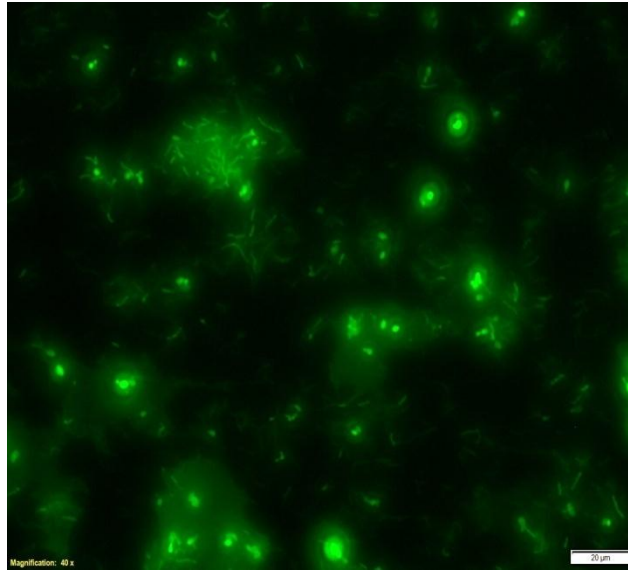


Figure 9.1: Bacterial Smear showing the FITC stained *Mycobacterium* at 40X.

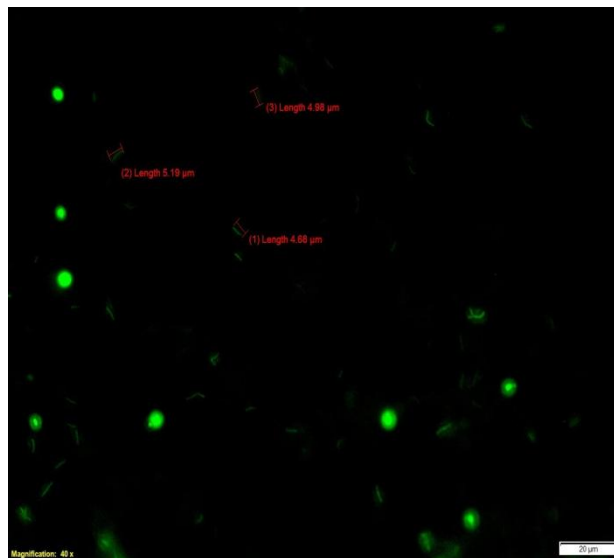


Figure 9.2: Fluorescent microscopy images of *Mycobacterium* bacteria on an agarose pad at 40X.

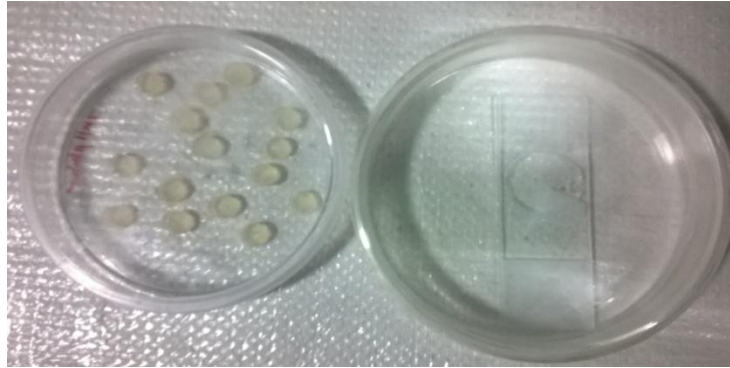


Figure 9.3: Types of Agarose pads used in this experiment

Discussion:

This experiment has been performed to learn and standardise the microscopy settings for imaging FITC stained bacterium. The results validated that it was possible to identify and image single bacterial cells once they had been FITC-stained by using a fluorescent microscope alone. This was an important intermediate result, as it proved that the devices could be imaged without a confocal microscope, thereby allowing greater ease of access and operation for future work.

2. Soft Lithography and Microfluidic Device Fabrication Experiments:

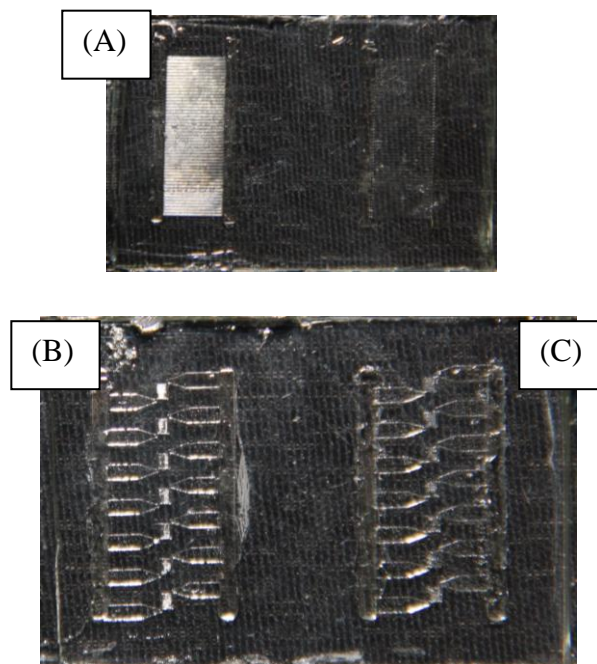


Figure 9.4: Images of the PDMS devices cast from the master moulds, taken by high resolution photography. A, B and C: first design, fourth and third design respectively. (Second design is not distinguishable).

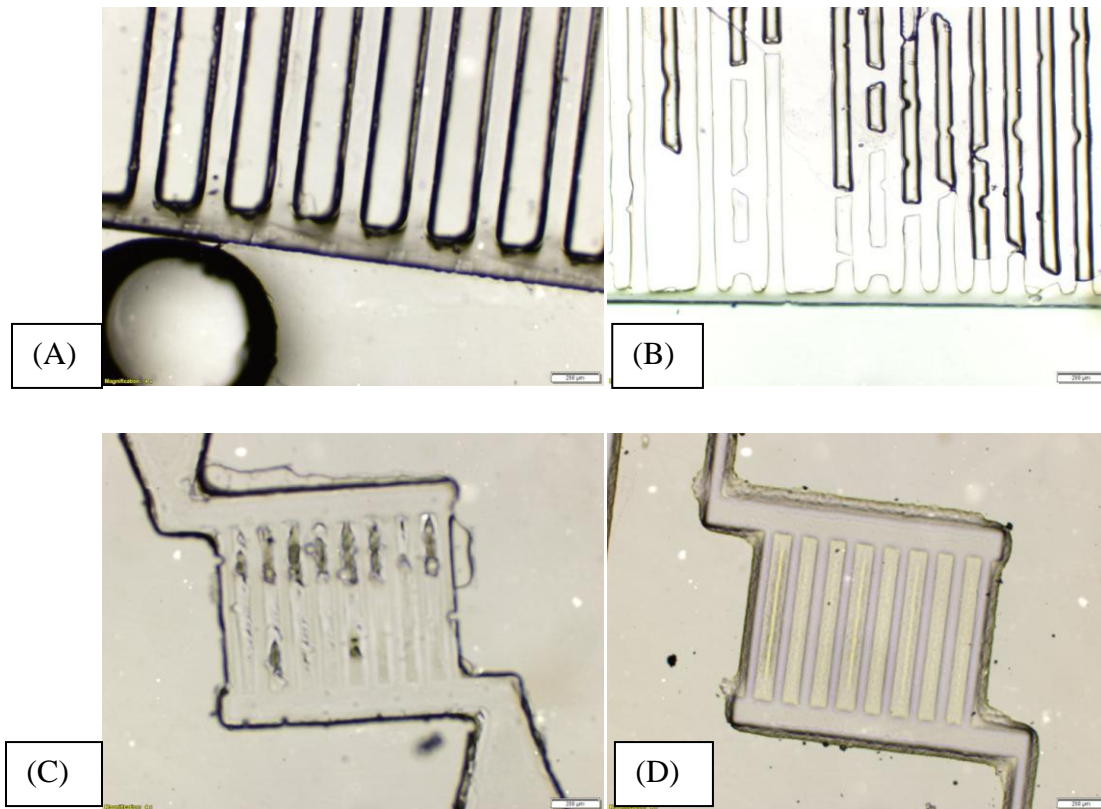


Figure 9.5: Bright field microscopy images of central chamber of all the four designs at 4X magnification. A, B, C and D correspond to that of the design no.1 2, 3 and 4 respectively.

Discussion:

From the above figure it can be seen that in design no.1 the central channels are offset from the inlet and outlet chambers. In the PDMS cast devices for design no.2, the central channels are broken in between. This can be attributed to fabrication errors during manual alignment of the photomask during UV exposure of the photoresist on the mould and due to improper baking during soft lithography process respectively.

It is evident from the above figure that the central isolation channels in the designs 3 and 4 are intact and workable, so the third design was utilized for the proof-of-concept experiments. However, given the time constraints, evaluation of the fourth design was out of the scope of the current project, and has been deferred for future work.

3. Fluorescent microscopy Imaging in Microfluidic Devices



Figure 9.6: Image of the complete Device no.3 with inlet and outlet tubing.

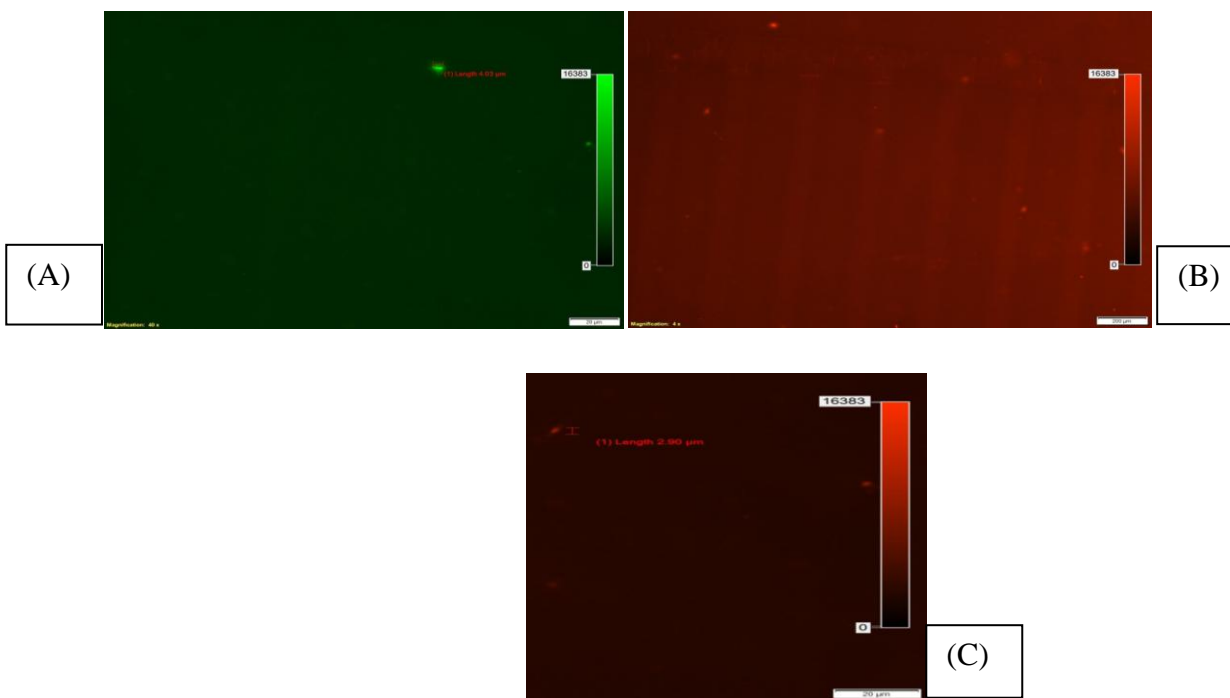


Figure 9.7: Fluorescent microscopy images in a microfluidic device. (A) FITC stained single *Mycobacterium* at 40 X. (B and C): mCherry strain *Mycobacterium* at 4X and 40 X respectively.

Discussion:

From the above microscopic images it can be concluded that by using design No. 3, single bacterium can be isolated upon injection of 25 micro-liter of the bacterial solution in one minute.

Chapter 10. PROOF OF CONCEPT

As a proof-of-concept to establish the utility of the present set of devices for studying morphological changes in *Mycobacteria*, the model system of *E. coli* has been used. This is because *E. coli* has a shorter replication time of 15-20 minutes as compared to *M. Tb* and it can replicate even at room temperature. Therefore, experiments to isolate and observe growth of *E. coli* under normal LB medium and after Kanamycin challenge have been performed

10.1. Evaluation of Bacterial Growth Under Normal Growth Conditions:

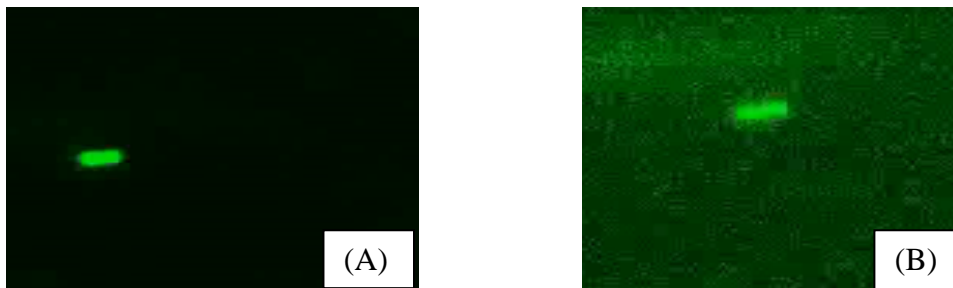


Figure 10.1: Fluorescent microscopy images at 40X of FITC stained *E. coli* under normal LB medium. (A and B) Images taken from the video generated by the microscope in an interval of ten minutes respectively.

Discussion:

In the above images it can be clearly observed that there is no change in morphology of the bacterium while it is dividing in the normal growth medium per se.

10.2. Evaluation of Bacterial Growth Under 25 $\mu\text{g/ml}$ Kanamycin in LB medium:

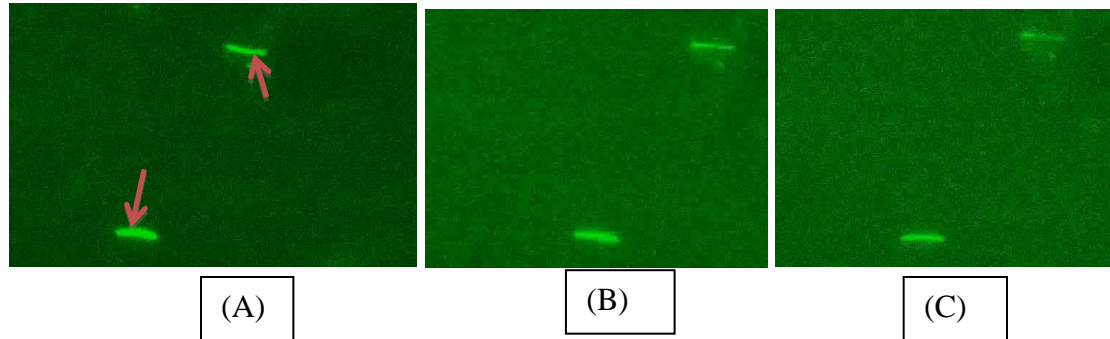


Figure 10.2: Fluorescent microscopic images of *E.coli* under Kanamycin (25 $\mu\text{g/ml}$) containing medium in the device at 40X. (A, B and C) Images from a video taken at an interval of 0, 5 and 10 minutes interval showing that the bacteria is attaining a filamentous form, a probable change in morphology due to the drug affecting the cellular physiology.

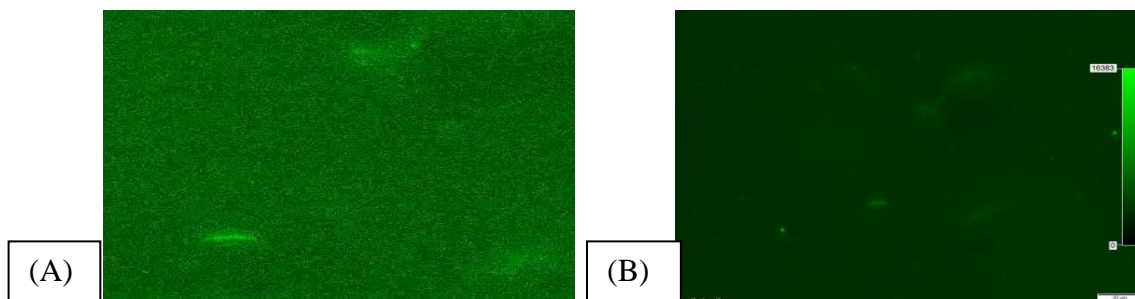


Figure 10.3: Fluorescent microscopic images of *E.coli* under Kanamycin (25 $\mu\text{g/ml}$) containing medium in the device after 30 minutes at 40 X. (A) A still shot from a time-lapse video in the last of the 30 minutes where the bacteria is seen waning out. (B) Fluorescent microscopic image of the same process.

10.3. Evaluation of Bacterial Growth Under 50 µg/ml Kanamycin in LB medium:

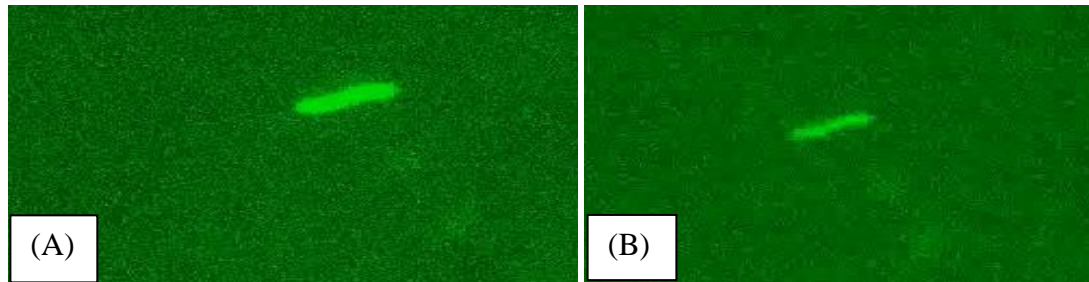


Figure 10.4: Fluorescent microscopic images of *E. coli* (O.D. - 0.2) under Kanamycin (50µg/ml) containing medium in the device at 40X. (A and B): Images at 0 and 10 minutes respectively. Here the bacterium is seen thinning at an interval of ten minutes.

Discussion:

Kanamycin is known to deregulate the protein synthesis by acting as an inhibitor to 30S ribosomal fragment. So the cell wall is dividing but probably it lacks other necessary proteins to complete its division process and other metabolic activities and hence thinning out.

Chapter 11. CONCLUSIONS AND FUTURE WORK

This project helped me in learning the basics of computer-aided engineering design using softwares like SolidWorks™ and AUTO CAD™. Further, the project provided an opportunity to learn and manufacture those designs by the application of soft lithography and microfabrication techniques. In this project, I had developed a protocol for live staining of the bacteria with a fluorescent dye, FITC. This has been done to study the morphological changes occurring in an isolated bacterium while it is dividing in the normal state and under other stress conditions such as antibiotic treatments.

Through the application of the microfabricated device, the isolation of a single bacterium has been successfully demonstrated. Further, in order to image the bacterium, high resolution fluorescent microscopy has been used. The microscopy images provided a proof of concept that the device can be used study to the morphological changes in single cells when grown in normal and drug containing medium. For this purpose *E.coli* has been used because it has short dividing time of 20 minutes so it was possible to image a probable morphological change taking place in a bacterium during its division.

The fabricated designs can be further used to study the effect various drugs upon the motility of the bacteria. The results shown in this work successfully demonstrated that the device was able to maintain cell viability and to observe motility on a time scale greater than a single cell cycle. This data can be extrapolated or co-related to the study of cell death induced in the bacterium by different drugs thus giving the information regarding the sensitivity and susceptibility to the drugs.

The device can also be used as a platform to study the bacterial replication and cell death under different conditions such as:

1. Under normal growth media.
2. Hypothermia/Hyperthermia.
3. Acidic/Basic pH.
4. Upon agarose+7H9/PDMS base micro-fluidic device.
5. Under different drugs and their different in-vitro concentrations.

All the above data can be used to study the factors that affect the bacterial growth when in different conditions/organs of the human body or in the external environment.

FUTURE DIRECTIONS:

1. The characterization of the device's fine structures and their fidelity to the desired dimension has to be confirmed through profilometry and scanning electron microscopy. This will help to optimize flow using inertial fluid focusing for single cell isolation and maintenance of cell viability.
2. Improving the time scale for maintaining cell viability for three to four cycles of cell division. This will provide the required complexity of truly evaluating the biological activity, morphological changes and emergence of phenotypic variations in isolated cells.
3. Simultaneous evaluation of all 4 designs to understand and identify the effects of differences in flow and changes in local cellular environment.
4. Perform statistical analysis to confirm the growth rate, size, death rate, etc. to analyze the data for the given set of divisions.

Chapter 12. REFERENCES

1. Avery SV (2006) Microbial cell individuality and the underlying sources of heterogeneity. *Nat Rev Microbiol* 4:577–587.
2. Dhar N, McKinney JD (2007) Microbial phenotypic heterogeneity and antibiotic tolerance. *Curr Opin Microbiol* 10:30–38.
3. Balaban NQ, Merrin J, Chait R et al (2004) Bacterial persistence as a phenotypic switch. *Science* 305:1622–1625.
4. Eldar A, Chary VK, Xenopoulos P et al (2009) Partial penetrance facilitates developmental evolution in bacteria. *Nature* 460:510–514.
5. Eldar A, Elowitz MB (2010) Functional roles for noise in genetic circuits. *Nature* 467:167–173.
6. Locke JC, Young JW, Fontes M et al (2011) Stochastic pulse regulation in bacterial stress response. *Science* 334:366–369.
7. Norman TM, Lord ND, Paulsson J et al (2013) Memory and modularity in cell-fate decision making. *Nature* 503:481–486.
8. Rotem E, Loinger A, Ronin I et al (2010) Regulation of phenotypic variability by a threshold-based mechanism underlies bacterial persistence. *Proc Natl Acad Sci U S A* 107:12541–12546.
9. Wakamoto Y, Dhar N, Chait R et al (2013) Dynamic persistence of antibiotic-stressed mycobacteria. *Science* 339:91–95.
10. Brehm-Stecher BF, Johnson EA (2004) Single-cell microbiology: tools, technologies, and applications. *Microbiol Mol Biol Rev* 68:538–559.
11. Ackermann M, Stearns SC, Jenal U (2003) Senescence in a bacterium with asymmetric division. *Science* 300:1920.
12. De Jong IG, Beilharz K, Kuipers OP, Veening J-W (2011) Live cell imaging of *Bacillus subtilis* and *Streptococcus pneumoniae* using automated time-lapse microscopy. *J Vis Exp* 53:e3145.
13. Golding I, Paulsson J, Zawilski SM et al (2005) Real-time kinetics of gene activity in individual bacteria. *Cell* 123:1025–1036.

14. Lindner AB, Madden R, Demarez A et al (2008) Asymmetric segregation of protein aggregates is associated with cellular aging and rejuvenation. *Proc Natl Acad Sci U S A* 105:3076–3081.
15. Locke JCW, Elowitz MB (2009) Using movies to analyse gene circuit dynamics in single cells. *Nat Rev Micro* 7:383–392.
16. Stewart EJ, Madden R, Paul G et al (2005) Aging and death in an organism that reproduces by morphologically symmetric division. *PLoS Biol* 3:e45
17. Wang P, Robert L, Pelletier J et al (2010) Robust growth of *Escherichia coli*. *Curr Biol* 20:1099–1103.
18. Young JW, Locke JC, Altinok A et al (2012) Measuring single-cell gene expression dynamics in bacteria using fluorescence time-lapse microscopy. *Nat Protoc* 7:80–88.
19. Aldridge BB, Fernandez-Suarez M, Heller D et al (2012) Asymmetry and aging of mycobacterial cells lead to variable growth and antibiotic susceptibility. *Science* 335:100–104.
20. Golchin SA, Stratford J, Curry RJ et al (2012) A microfluidic system for long-term time-lapse microscopy studies of mycobacteria. *Tuberculosis (Edinb)* 92:489–496.
21. Joyce G, Robertson BD, Williams KJ (2011) A modified agar pad method for mycobacterial live-cell imaging. *BMC Res Notes* 4:73.
22. Dino Di Carlo, Inertial microfluidic, *Lab Chip*, 2009, 9, 3038–3046.
23. Ali Asgar S. Bhagat et al, *Physics of Fluids*, Enhanced particle filtration in straight microchannels using shear-modulated inertial migration, 20, 101702, 2008.